Published OnlineFirst September 16, 2014; DOI: 10.1158/1078-0432.CCR-14-1511

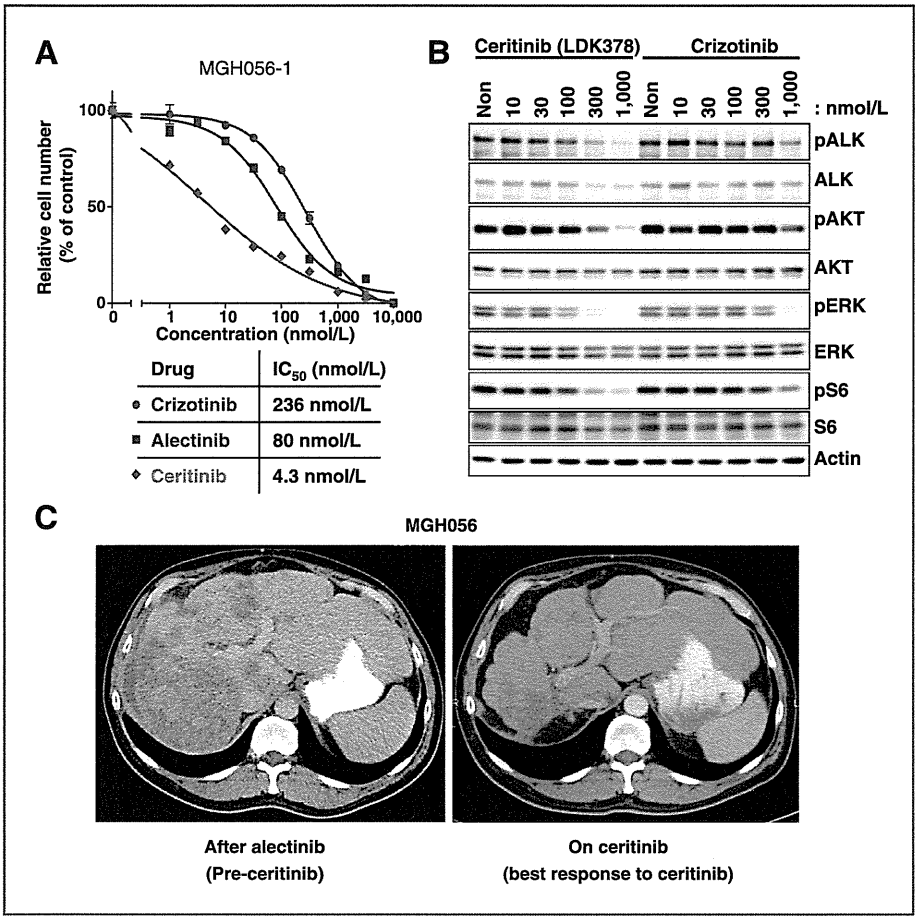

Figure 5. Preclinical and clinical activity of ceritinib in alectinib-resistant cancer cells harboring the I1171T mutation. A, MGH056-1 cells were seeded in 96-well plates and treated with the indicated concentration of crizotinib, alectinib, or ceritinib for 72 hours. Cell viability was measured using the CellTiter-Glo Assay. B, MGH056 cells were exposed to increasing concentrations of crizotinib or ceritinib for 6 hours. Cell lysates were immunoblotted to detect the indicated proteins. C, axial CT scan images of patient MGH056. Left, an axial slice through this patient's liver after he had relapsed on alectinib and before ceritinib. Right, a comparable axial image after 18 weeks of ceritinib treatment demonstrating marked improvement in his liver metastases.

phosphorylation and downstream AKT and ERK phosphorylation to a greater extent than crizotinib and alectinib (Figs. 5B and 2C). Consistent with these results, treatment of patient MGH056 with ceritinib led to significant tumor regression (Fig. 5C), with a confirmed partial response lasting over 7 months. These preclinical and clinical results suggest that ceritinib may be effective in treating cancers that have become resistant to alectinib due to a secondary mutation such as I1171T or V1180L.

Discussion

ALK-rearranged NSCLC represents one of the newest oncogene-addiction paradigms in clinical oncology. As with other oncogene-addicted cancers, ALK-rearranged lung cancers are initially sensitive to the first-generation targeted agent, but eventually become resistant through a variety of different mechanisms. Remarkably, the vast majority of crizotinib-resistant tumors remain ALK-dependent and re-respond to more potent, next-generation ALK inhibitors such as alectinib and ceritinib (21, 31). However, despite their promising activity in early-phase studies, resistance to next-generation ALK inhibitors invariably develops and ultimately limits the clinical benefit afforded by these new agents.

In this study, we focused on acquired resistance to alectinib, one of the most advanced of the next-generation ALK inhibitors in the clinic. We identified two novel ALK mutations, V1180L in a cell line made resistant to alectinib, and I1171T in a tumor specimen from a patient who had relapsed on alectinib. Both mutations confer resistance to crizotinib as well as alectinib, and hence add to the growing list of secondary *ALK* mutations that can mediate crizotinib resistance. Mutation of the V1180 residue has not yet been reported in patients, but was observed at very low frequency in an *in vitro* mutagenesis screen for crizotinib-resistant mutants in *EML4-ALK* (25). On the basis of the crystal structure of ALK (32), V1180 resides at the back of the ATP pocket and likely makes direct contact with crizotinib and alectinib, similar to the L1196 gatekeeper residue. Our computational modeling revealed weaker binding of alectinib to the V1180L-mutant compared with WT ALK, supporting the notion that substitution of leucine for valine at this residue interferes with the ability of alectinib to bind effectively to the kinase.

The second alectinib-resistant mutation, I1171T, has not been previously reported in crizotinib-resistant patients, but mutation of this residue has been described in 2 patients with neuroblastoma (26). In neuroblastoma, mutation at

Published OnlineFirst September 16, 2014; DOI: 10.1158/1078-0432.CCR-14-1511

this residue results in an I1171N amino substitution and leads to activation of ALK, though the mutant kinase is unable to transform Ba/F3 cells (33). On the basis of our computational modeling studies, we would predict that I1171T disrupts a hydrogen bond between alectinib and E1167 (Fig. 3D), destabilizing the complex of alectinib with the mutant kinase. Whether ALK I1171T is weakly oncogenic like I1171N and whether this could contribute to crizotinib resistance is unknown.

Compared with V1180L, which conferred high-level TKI resistance, the I1171T mutation was associated with intermediate resistance to alectinib in cell line studies. This mutation was discovered in a patient who had relapsed after 4 months of alectinib therapy. Before alectinib, the patient had received crizotinib with a response lasting 8 months. Although no tumor specimens were available before or after crizotinib therapy for genetic analyses, we suspect that the I1171T mutation emerged during the course of alectinib treatment, given his previous durable response to crizotinib followed by a re-response to alectinib. Of note, this patient was treated with alectinib at a dose of 300 mg twice daily. This represents half of the recommended phase II dose (RP2D) of alectinib established in a recent phase I study (NCT01588028; ref. 20). The relatively low drug exposure at this dose may have been a factor in selecting and/or expanding a clone with intermediate resistance to alectinib. As higher drug exposures are predicted at the RP2D, we speculate that patients treated at this dose could develop more highly resistant mutations such as V1180L.

Recently, several other mechanisms of resistance have been reported in patients who have relapsed on next-generation ALK inhibitors. The solvent front mutation G1202R, first discovered in a crizotinib-resistant tumor (11), appears to mediate high-level resistance to both alectinib and ceritinib. In one case, a patient who had relapsed on crizotinib was treated with alectinib at the RP2D and showed no evidence of response, consistent with intrinsic resistance (34). Molecular studies performed on a resistant specimen revealed the G1202R mutation. Similarly, in a series of 11 ceritinib-resistant tumors, three were found to harbor a new G1202R mutation and two had acquired a mutation at residue F1174 (17). Importantly, neither of these mutations was detectable in biopsies taken before ceritinib treatment. In the absence of a secondary *ALK* mutation, activation of alternative signaling pathways could also mediate resistance to alectinib. Indeed, in 1 patient who had relapsed on alectinib, amplification of *cMET* was reported in a resistant specimen, although it is unknown if it was driving resistance (35). In the case of our alectinib-resistant patient with I1171T, cMET was likely not driving the development of resistance, because ceritinib, which has no anti-cMET activity, was able to induce a durable response lasting over 7 months.

The observation that other structurally distinct, next-generation ALK inhibitors may overcome alectinib resistance *in vitro* and *in vivo* is clinically significant. Currently, nine next-generation ALK inhibitors have entered the clinic, with several showing potent activity in both crizotinib-naïve and crizotinib-resistant patients (19–21). One of the nine next-generation ALK inhibitors has already been approved by the U.S. FDA for the treatment of advanced, crizotinib-resistant, ALK-positive NSCLC. Until now, it was unknown whether patients could continue to derive benefit from ALK inhibition after failure of a next-generation ALK inhibitor. Our results suggest that patients may benefit from multiple, sequential ALK inhibitor therapies, depending on the underlying mechanism of resistance. In those cases with susceptible resistance mutations, such as V1180L and I1171T, ceritinib may be highly effective, even in a third-line, post-crizotinib, post-alectinib setting. However, in cases where resistance is mediated by a highly recalcitrant mutation, such as G1202R or by a completely different tyrosine kinase, ceritinib may not be helpful, and alternative treatment strategies, such as hsp90 inhibition or combinatorial therapeutics, may be required. Overall, these findings highlight the importance of serial biopsies to track the dynamic evolution of drug resistance, and to enable the rational selection of therapies most likely to be effective based on the underlying molecular alterations.

Disclosure of Potential Conflicts of Interest

J. Iafrate is a consultant/advisory board member for Chugai and Pfizer. K. Takeuchi is a consultant/advisory board member for and reports receiving a commercial research grant and speakers bureau honoraria from Chugai. J.A. Engelman reports receiving a commercial research grant from Novartis and is a consultant/advisory board member for Chugai, Genentech, Novartis, and Ventana. A.T. Shaw is a consultant/advisory board member for Ignyta, Genentech, Novartis, and Pfizer. No potential conflicts of interest were disclosed by the other authors.

Authors' Contributions

Conception and design: R. Katayama, N. Fujita, J.A. Engelman, A.T. Shaw
Development of methodology: R. Katayama
Acquisition of data (provided animals, acquired and managed patients, provided facilities, etc.): R. Katayama, L. Friboulet, S. Koike, E.L. Lockerman, T.M. Khan, J.F. Gainor, A.J. Iafrate, A.T. Shaw
Analysis and interpretation of data (e.g., statistical analysis, biostatistics, computational analysis): R. Katayama, S. Koike, J.F. Gainor, A.J. Iafrate, K. Takeuchi, Y. Okuno, N. Fujita, J.A. Engelman, A.T. Shaw
Writing, review, and/or revision of the manuscript: R. Katayama, J.F. Gainor, A.J. Iafrate, Y. Okuno, N. Fujita, J.A. Engelman, A.T. Shaw
Administrative, technical, or material support (i.e., reporting or organizing data, constructing databases): R. Katayama, S. Koike, M. Taiji, N. Fujita
Study supervision: N. Fujita, J.A. Engelman, A.T. Shaw

Acknowledgments

The authors thank S. Baba at the Japanese Foundation for Cancer Research (JFCR) for helping with the FISH analysis. Use of the "K" Supercomputer from RIKEN is also acknowledged.

Grant Support

The study was supported, in part, by R01CA137008, R01CA140594, National Cancer Institute Lung SPORE (to J.A. Engelman), R01CA164273 (to A.T. Shaw and J.A. Engelman) and JSPS KAKENHI grant number 24300344 and 22112008 (to N. Fujita) and 25710015 (to R. Katayama).

The costs of publication of this article were defrayed in part by the payment of page charges. This article must therefore be hereby marked *advertisement* in accordance with 18 U.S.C. Section 1734 solely to indicate this fact.

Received June 13, 2014; revised August 6, 2014; accepted August 9, 2014; published OnlineFirst September 16, 2014.

Published OnlineFirst September 16, 2014; DOI: 10.1158/1078-0432.CCR-14-1511

References

1. Soda M, Choi YL, Enomoto M, Takada S, Yamashita Y, Ishikawa S, et al. Identification of the transforming EML4-ALK fusion gene in non–small-cell lung cancer. Nature 2007;448:561–6.
2. Takeuchi K, Choi YL, Togashi Y, Soda M, Hatano S, Inamura K, et al. KIF5B-ALK, a novel fusion oncokinase identified by an immunohistochemistry-based diagnostic system for ALK-positive lung cancer. Clin Cancer Res 2009;15:3143–9.
3. Takeuchi K, Soda M, Togashi Y, Ota Y, Sekiguchi Y, Hatano S, et al. Identification of a novel fusion, SQSTM1-ALK, in ALK-positive large B-cell lymphoma. Haematologica 2011;96:464–7.
4. Togashi Y, Soda M, Sakata S, Sugawara E, Hatano S, Asaka R, et al. KLC1-ALK: a novel fusion in lung cancer identified using a formalin-fixed paraffin-embedded tissue only. PLoS ONE 2012;7:e31323.
5. Shaw AT, Hsu PP, Awad MM, Engelman JA. Tyrosine kinase gene rearrangements in epithelial malignancies. Nat Rev Cancer 2013;13:772–87.
6. Camidge DR, Bang YJ, Kwak EL, Iafrate AJ, Varella-Garcia M, Fox SB, et al. Activity and safety of crizotinib in patients with ALK-positive non–small-cell lung cancer: updated results from a phase 1 study. Lancet Oncol 2012;13:1011–9.
7. Kwak EL, Bang YJ, Camidge DR, Shaw AT, Solomon B, Maki RG, et al. Anaplastic lymphoma kinase inhibition in non–small-cell lung cancer. N Engl J Med 2010;363:1693–703.
8. Shaw AT, Kim DW, Nakagawa K, Seto T, Crino L, Ahn MJ, et al. Crizotinib versus chemotherapy in advanced ALK-positive lung cancer. N Engl J Med 2013;368:2385–94.
9. Choi YL, Soda M, Yamashita Y, Ueno T, Takashima J, Nakajima T, et al. EML4-ALK mutations in lung cancer that confer resistance to ALK inhibitors. N Engl J Med 2010;363:1734–9.
10. Katayama R, Khan TM, Benes C, Lifshits E, Ebi H, Rivera VM, et al. Therapeutic strategies to overcome crizotinib resistance in non–small cell lung cancers harboring the fusion oncogene EML4-ALK. Proc Natl Acad Sci U S A 2011;108:7535–40.
11. Katayama R, Shaw AT, Khan TM, Mino-Kenudson M, Solomon BJ, Halmos B, et al. Mechanisms of acquired crizotinib resistance in ALK-rearranged lung Cancers. Sci Transl Med 2012;4:120ra17.
12. Sasaki T, Okuda K, Zheng W, Butrynski J, Capelletti M, Wang L, et al. The neuroblastoma-associated F1174L ALK mutation causes resistance to an ALK kinase inhibitor in ALK-translocated cancers. Cancer Res 2010;70:10038–43.
13. Sasaki T, Koivunen J, Ogino A, Yanagita M, Nikiforow S, Zheng W, et al. A novel ALK secondary mutation and EGFR signaling cause resistance to ALK kinase inhibitors. Cancer Res 2011;71:6051–60.
14. Doebele RC, Pilling AB, Aisner DL, Kutateladze TG, Le AT, Weickhardt AJ, et al. Mechanisms of resistance to crizotinib in patients with ALK gene rearranged non–small cell lung cancer. Clin Cancer Res 2012;18:1472–82.
15. Lovly CM, Pao W. Escaping ALK inhibition: mechanisms of and strategies to overcome resistance. Sci Transl Med 2012;4:120ps2.
16. Kim S, Kim TM, Kim DW, Go H, Keam B, Lee SH, et al. Heterogeneity of genetic changes associated with acquired crizotinib resistance in ALK-rearranged lung cancer. J Thorac Oncol 2013;8:415–22.
17. Friboulet L, Li N, Katayama R, Lee CC, Gainor JF, Crystal AS, et al. The ALK inhibitor ceritinib overcomes crizotinib resistance in non–small cell lung cancer. Cancer Discov 2014;4:662–73.
18. Sakamoto H, Tsukaguchi T, Hiroshima S, Kodama T, Kobayashi T, Fukami TA, et al. CH5424802, a selective ALK inhibitor capable of blocking the resistant gatekeeper mutant. Cancer Cell 2011;19:679–90.
19. Seto T, Kiura K, Nishio M, Nakagawa K, Maemondo M, Inoue A, et al. CH5424802 (RO5424802) for patients with ALK-rearranged advanced non–small-cell lung cancer (AF-001JP study): a single-arm, open-label, phase 1–2 study. Lancet Oncol 2013;14:590–8.
20. Ou SH, Gadgeel S, Chiappori A, Riely G, Lee R, Garcia L, et al. Safety and efficacy analysis of RO5424802/CH5424802 in anaplastic lymphoma kinase (ALK)-positive non–small cell lung cancer (NSCLC) patients who have failed crizotinib in a dose-finding phase I study (AF-002JG, NCT01588028). In: Proceedings of The European Cancer Congress; 2013 September 30; Basel, Switzerland. Abstract nr 44 LBA.
21. Shaw AT, Kim DW, Mehra R, Tan DS, Felip E, Chow LQ, et al. Ceritinib in ALK-rearranged non–small-cell lung cancer. N Engl J Med 2014;370:1189–97.
22. Koivunen JP, Mermel C, Zejnullahu K, Murphy C, Lifshits E, Holmes AJ, et al. EML4-ALK fusion gene and efficacy of an ALK kinase inhibitor in lung cancer. Clin Cancer Res 2008;14:4275–83.
23. Ono M, Hirata A, Kometani T, Miyagawa M, Ueda S, Kinoshita H, et al. Sensitivity to gefitinib (Iressa, ZD1839) in non–small cell lung cancer cell lines correlates with dependence on the epidermal growth factor (EGF) receptor/extracellular signal-regulated kinase 1/2 and EGF receptor/Akt pathway for proliferation. Mol Cancer Ther 2004;3:465–72.
24. Amann J, Kalyankrishna S, Massion PP, Ohm JE, Girard L, Shigematsu H, et al. Aberrant epidermal growth factor receptor signaling and enhanced sensitivity to EGFR inhibitors in lung cancer. Cancer Res 2005;65:226–35.
25. Zhang S, Wang F, Keats J, Zhu X, Ning Y, Wardwell SD, et al. Crizotinib-resistant mutants of EML4-ALK identified through an accelerated mutagenesis screen. Chem Biol Drug Des 2011;78:999–1005.
26. Mosse YP, Laudenslager M, Longo L, Cole KA, Wood A, Attiyeh EF, et al. Identification of ALK as a major familial neuroblastoma predisposition gene. Nature 2008;455:930–5.
27. Fujitani H, Tanida Y, Matsuura A. Massively parallel computation of absolute binding free energy with well-equilibrated states. Phys Rev E Stat Nonlin Soft Matter Phys 2009;79:021914.
28. Galkin AV, Melnick JS, Kim S, Hood TL, Li N, Li L, et al. Identification of NVP-TAE684, a potent, selective, and efficacious inhibitor of NPM-ALK. Proc Natl Acad Sci U S A 2007;104:270–5.
29. Sang J, Acquaviva J, Friedland JC, Smith DL, Sequeira M, Zhang C, et al. Targeted inhibition of the molecular chaperone Hsp90 overcomes ALK inhibitor resistance in non–small cell lung cancer. Cancer Discov 2013;3:430–43.
30. Sequist LV, Gettinger S, Senzer NN, Martins RG, Janne PA, Lilenbaum R, et al. Activity of IPI-504, a novel heat-shock protein 90 inhibitor, in patients with molecularly defined non–small-cell lung cancer. J Clin Oncol 2010;28:4953–60.
31. Awad MM, Katayama R, McTigue M, Liu W, Deng YL, Brooun A, et al. Acquired resistance to crizotinib from a mutation in CD74-ROS1. N Engl J Med 2013;368:2395–401.
32. Bossi RT, Saccardo MB, Ardini E, Menichincheri M, Rusconi L, Magnaghi P, et al. Crystal structures of anaplastic lymphoma kinase in complex with ATP competitive inhibitors. Biochemistry 2010;49:6813–25.
33. Schonherr C, Ruuth K, Yamazaki Y, Eriksson T, Christensen J, Palmer RH, et al. Activating ALK mutations found in neuroblastoma are inhibited by crizotinib and NVP-TAE684. Biochem J 2011;440:405–13.
34. Ou SH, Azada M, Hsiang DJ, Herman JM, Kain TS, Siwak-Tapp C, et al. Next-generation sequencing reveals a Novel NSCLC ALK F1174V mutation and confirms ALK G1202R mutation confers high-level resistance to alectinib (CH5424802/RO5424802) in ALK-rearranged NSCLC patients who progressed on crizotinib. J Thorac Oncol 2014;9:549–53.
35. Gouji T, Takashi S, Mitsuhiro T, Yukito I. Crizotinib can overcome acquired resistance to CH5424802: is amplification of the MET gene a key factor? J Thorac Oncol 2014;9:e27–8.

Cancer Science
Japanese Cancer Association JCA
Open Access

Platelets promote osteosarcoma cell growth through activation of the platelet-derived growth factor receptor-Akt signaling axis

Satoshi Takagi, Ai Takemoto, Miho Takami, Tomoko Oh-hara and Naoya Fujita

Division of Experimental Chemotherapy, Cancer Chemotherapy Center, Japanese Foundation for Cancer Research, Tokyo, Japan

Key words

Akt, osteosarcoma, platelet aggregation, platelet derived growth factor receptor, tumor-platelet interaction

Correspondence

Naoya Fujita, Cancer Chemotherapy Center, Japanese Foundation for Cancer Research, Tokyo 135-8550, Japan.
Tel: +81-3-3570-0468; Fax: +81-3-3570-0484;
E-mail: naoya.fujita@jfcr.or.jp

Funding information

National Institute of Biomedical Innovation (NIBIO) (to NF). Ministry of Education, Culture, Sports, Science, and Technology of Japan (to NF and ST).

Received March 19, 2014; Revised April 16, 2014; Accepted June 8, 2014

Cancer Sci **105** (2014) 983–988

doi: 10.1111/cas.12464

The interactions of tumor cells with platelets contribute to the progression of tumor malignancy, and the expression levels of platelet aggregation-inducing factors positively correlate with the metastatic potential of osteosarcoma cells. However, it is unclear how tumor-platelet interaction contributes to the proliferation of osteosarcomas. We report here that osteosarcoma-platelet interactions induce the release of platelet-derived growth factor (PDGF) from platelets, which promotes the proliferation of osteosarcomas. Co-culture of platelets with MG63 or HOS osteosarcoma cells, which could induce platelet aggregation, enhanced the proliferation of each cell line *in vitro*. Analysis of phospho-antibody arrays revealed that co-culture of MG63 cells with platelets induced the phosphorylation of platelet derived growth factor receptor (PDGFR) and Akt. The addition of supernatants of osteosarcoma-platelet reactants also increased the growth of MG63 and HOS cells as well as the level of phosphorylated-PDGFR and -Akt. Sunitinib or LY294002, but not erlotinib, significantly inhibited the platelet-induced proliferation of osteosarcoma cells, indicating that PDGF released from platelets plays an important role in the proliferation of osteosarcomas by activating the PDGFR and then Akt. Our results suggest that inhibitors that specifically target osteosarcoma-platelet interactions may eradicate osteosarcomas.

Osteosarcoma is the most common primary malignant bone tumor of children and adolescents and is derived from primitive mesenchymal cells.[1] This disease is highly aggressive, and distant metastasis develop in approximately 45% of patients despite treatment with a potent neoadjuvant, which consists of high doses of multiple chemotherapeutic agents.[2] Approximately 20% of patients have metastatic sites in the lungs or bones at diagnosis [3] and have a poor prognosis despite aggressive surgery and chemotherapy.[4] Thus, more effective therapeutic approaches are required for treating these patients.

The interactions of tumor cells with platelets play a critical role in the progression of tumor malignancy. Tumor cell-induced platelet aggregation enhances the rate of tumor embolization in the microvasculature and protects tumor cells from immunological assault and blood-shear stress.[5] Moreover, several factors such as transforming growth factor-β, vascular endothelial growth factor, and platelet-derived growth factor (PDGF) are stored in platelet granules and are released during platelet aggregation.[6,7] Such platelet-derived factors promote the epithelial-mesenchymal transition, tumor vascular angiogenesis, and vascular permeability.[8,9] Further, experimentally induced thrombocytopenia and antiplatelet agents decrease the rate of lung metastasis in mouse models, indicating the requirement for platelets in the formation of hematogenous metastasis.[10–12]

Osteosarcoma cells possess the potential to induce platelet aggregation, and there is positive correlation between the expression level of platelet aggregation-inducing factors and the potential of osteosarcomas to metastasize to the lungs.[13] However, the effect of osteosarcoma-platelet interactions on the proliferation of osteosarcoma cells is unknown. We report here that osteosarcoma-platelet interactions induce the release of PDGF from platelets and enhance the proliferation of osteosarcomas. Co-culture of osteosarcoma cells with platelets promoted the proliferation of osteosarcoma cells. Analysis of phospho-antibody arrays revealed that the osteosarcoma-platelet interaction increased the phosphorylation of PDGFR and Akt. Using kinase inhibitors, phosphorylation of PDGFR and Akt were shown to be important for the platelet-dependent proliferation of osteosarcoma cells. These results suggest that osteosarcoma-platelet interactions initiate platelet aggregation, release PDGF from activated platelets, and activate the PDGFR-Akt signaling pathway to increase the growth of osteosarcoma cells.

Materials and Methods

Plasmid construction. The open reading frame (ORF) of a human codon-optimized variant of wild-type *Zoanthus* sp. green fluorescence protein (ZsGreen) was subcloned from the pZsGreen-N1 vector (Takara Bio, Shiga, Japan) into the pQCXIN retroviral vector (Takara Bio), and the resulting construct was designated pQCXIN-ZsGreen. Retroviral infection was performed according to the manufacturer's protocols.

Cell lines. The human osteosarcoma cell lines, MG63 and HOS, were purchased from the American Type Culture

Collection (ATCC, Manassas, VA, USA) and cultured in Dulbecco's modified Eagle's medium (DMEM, Sigma-Aldrich, St. Louis, MO, USA) containing 10% FBS (DMEM growth medium). MG63 and HOS cells that had stably transfected with *ZsGreen* gene (MG63/ZsGreen and HOS /ZsGreen, respectively) were cultured in DMEM growth medium containing 400 μg/mL of G418 (Life Technologies, Carlsbad, CA, USA).

Immunoblot analysis. Sample preparation was performed as described previously.[14] Briefly, cells were lysed in TENSV buffer (50 mM Tris–HCl (pH 7.5), 2 mM ethylenediaminetetraacetic acid (EDTA), 100 mM NaCl, 1 mM Na_3VO_4, 1% NP-40, 0.1% aprotinin, and 2 mM phenylmethylsulfonyl fluoride), and electrophoresed in sodium dodecyl sulfate (SDS)-polyacrylamide gel. The proteins were transferred to a membrane and immunoblotted with an anti-Akt (pan) monoclonal antibody (mAb) (clone C67E7, Cell Signaling Technology, Danvers, MA, USA), anti-phospho-Akt (Ser473) mAb (clone D9E, Cell Signaling Technology), anti-PDGFRβ polyclonal antibody (P-20, Santa Cruz Biotechnology, Santa Cruz, CA, USA), anti-phospho-PDGFRβ mAb (clone 42F9, Cell Signaling Technology), and anti-α-tubulin mAb (clone YL1/2, AbD Serotec, Kidlington, UK). The LAS-3000 mini system (Fujifilm, Tokyo, Japan) was used for visualization and quantification of signals.

Human phospho-RTK and human phospho-kinase arrays. Phosphorylation of signaling molecules was estimated using the Human Phospho-RTK Array Kit (ARY001B, R&D Systems, Minneapolis, MN, USA) and Human Phospho-Kinase Array Kit (ARY003B, R&D Systems) according to the manufacturer's protocols. Briefly, MG63 cells were co-cultured with buffer or platelets for 2 h. Three hundred micrograms of total cell lysates were incubated with each array. Proteins were detected using horse radish peroxidase (HRP)-conjugated mouse anti-phosphotyrosine antibody or streptavidin-HRP. Data were acquired using the LAS-3000 mini system. Image quantification was performed using Multi Gauge ver.3.0 software (Fujifilm). The signal intensities of duplicate spots were quantified.

Platelet preparation and aggregation assay. Whole blood was drawn by cardiac puncture from Jcl: ICR mice terminally anesthetized with chloroform and taken with 0.38% sodium citrate solution or 10 units/mL of heparin. The blood was centrifuged at 150 *g* for 8 min to obtain platelet-rich plasma (PRP) from the supernatant. Washed platelets were prepared from pellets of PRP by centrifugation at 500 *g* for 10 min following washing with modified Tyrode's buffer (137 mM NaCl, 11.9 mM $NaHCO_3$, 0.4 mM Na_2HPO_4, 2.7 mM KCl, 1.1 mM $MgCl_2$, and 5.6 mM glucose). Washed platelets were resuspended in modified Tyrode's buffer containing 1–2% murine platelet-poor plasma (PPP), and 200 or 250 μM $CaCl_2$ (each concentration used are shown in figure legends) was added to the platelet suspensions before starting the experiments. Platelet suspensions (200 μL) in the reaction tubes were stirred at 37°C and preincubated for 2 min before the addition of osteosarcoma cells. The platelet aggregation assay was performed using a platelet aggregometer (MCM HEMA TRACER 313M; SSR Engineering, Kanagawa, Japan) as previously described.[15]

Cell viability assay. MG63/ZsGreen and HOS/ZsGreen cells were suspended in DMEM medium containing 0.5% FBS (0.5×10^4 and 2.0×10^4 cells/mL, respectively) and seeded 0.1 mL in a 96-well plate. After overnight incubation, cells were co-cultured with washed platelets resuspended in modified Tyrode's buffer containing 200 μM $CaCl_2$. At the appropriate times, supernatants were removed, and TENSV buffer was added to the cultured cells. The fluorescence of ZsGreen in cell lysates was measured using a TriStar LB941 Multimode Microplate Reader (Berthold Technologies, Bad Wildbad, Germany). Buffer alone indicates the treatment of the cells with modified Tyrode's buffer containing 200 μM $CaCl_2$. In some experiments, the supernatant harvested from osteosarcoma-platelet reactants was added to the cultured osteosarcoma cells instead of platelets.

Preparation of supernatants of osteosarcoma cell-platelet reactants. Washed mouse platelets were prepared using 0.38% sodium citrate as described in the platelet preparation. Platelets (2.0×10^8 platelets/mL) were resuspended in modified Tyrode's buffer containing 1% murine PPP and 200 μM $CaCl_2$ and then incubated with phosphate-buffered saline (PBS) or osteosarcoma cells (2.5×10^5 cells/mL) for 30 min, at 37°C. After centrifuging twice at 10 000 *g* for 10 min, the supernatants of the reaction mixtures were designated PBS-platelet reactant and osteosarcoma-platelet reactant, respectively.

Animals. Jcl:ICR mice were purchased from Clea Japan (Tokyo, Japan). The animal procedures followed protocols approved by the Japanese Foundation for Cancer Research Animal Care and Use Committee.

Statistical analysis. The Student's *t*-test was performed to determine the statistical significance of the results of the proliferation assays. Significant *P*-values are defined as $^{**}P < 0.01$, $^{*}P < 0.05$. NS indicates a value that is not significant. All statistical tests were two-sided.

Results

Osteosarcoma-platelet interaction promotes platelet aggregation and osteosarcoma cell growth. Osteosarcomas form pulmonary metastasis by inducing platelet aggregation.[16,17] To assess the role of osteosarcoma-platelet interactions in determining the malignant phenotype of osteosarcomas, we first measured the abilities of the human osteosarcoma cell lines MG63 and HOS to induce platelet aggregation. We found that each osteosarcoma cell line induced platelet aggregation to an extent that is consistent with published studies (Fig. 1a). We next examined the influence of platelets on the growth of the osteosarcoma cell lines. Because of the high concentration of adenosine triphosphate (ATP) in platelets, we were unable to determine the growth of osteosarcoma cells using proliferation assays that measure ATP. Therefore, we generated stable transfectants of MG63 and HOS cells that expressed ZsGreen (MG63/ZsGreen and HOS/ZsGreen, respectively) and measured ZsGreen fluorescence to determine the number of viable cells. Although the growth rates of MG63/ZsGreen and HOS /ZsGreen cells were slow in the presence of 0.5% FBS, the growth rate of each cell line was significantly enhanced in proportion to the number of washed platelets added to the cultured cells (Fig. 1b). We found that the addition of the supernatant of an osteosarcoma-platelet reactant, but not that of the PBS-platelet reactant, significantly enhanced the growth of MG63/ZsGreen and HOS/ZsGreen cells (Fig. 1c). These results indicate that the proliferation of osteosarcoma cells is increased in the presence of platelets as well as by supernatants of osteosarcoma-platelet reactant.

Activation of the PDGFR-Akt axis in platelet-induced osteosarcoma proliferation. Platelets contain many growth factors and cytokines, including transforming growth factor-β, vascular endothelial growth factors, and PDGFs,[6,7] which are stored in platelet granules and released on platelet aggregation. Such platelet-derived factors promote the epithelial-mesenchymal transition, tumor vascular angiogenesis, and tumor growth.[8]

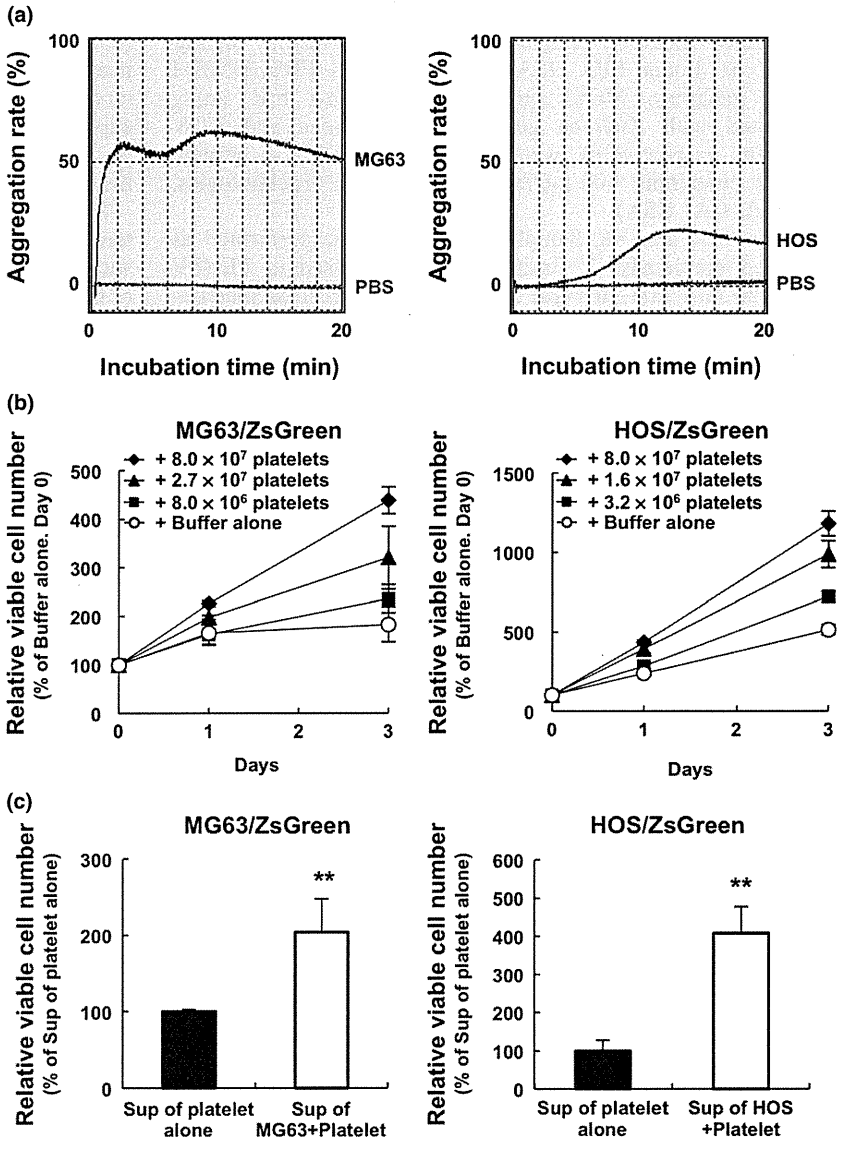

Fig. 1. Co-culture with platelets promotes platelet aggregation and the proliferation of osteosarcoma cells. (a) Platelets (4.0×10^7) prepared with heparin from the whole blood of Jcl:ICR mice were resuspended in modified Tyrode's buffer containing 2% PPP and 250 μM $CaCl_2$, followed by incubation with PBS (red lines) or osteosarcoma MG63 (left panel, black line) and HOS (right panel, black line) cells (1.0×10^8 cells). The transmission of light by the samples was measured using an aggregometer to determine the aggregation rate. (b) MG63 and HOS cells stably transfected with *ZsGreen* gene, MG63/ZsGreen (left panel) and HOS/ZsGreen (right panel), respectively, were co-cultured with the indicated number of washed mouse platelets in medium containing 0.5% FBS. TENSV buffer was added to each well at the times indicated, and the fluorescence of ZsGreen was used to determine the number of viable osteosarcoma cells. The error bars indicate the mean ± standard deviation (SD) of triplicate experiments. (c) Washed mouse platelets (2.0×10^7 platelets) were resuspended in modified Tyrode's buffer containing 1% PPP and 200 μM $CaCl_2$ followed by incubation with PBS or osteosarcoma cells (2.5×10^4 cells) for 30 min. After centrifugation twice at 10 000 *g* for 10 min, the supernatant of osteosarcoma-platelet reactants or the PBS-platelet reactant was added to the cultures of MG63/ZsGreen (left panel) and HOS /ZsGreen (right panel) cells. After 24 h, TENSV buffer was added to each well and the fluorescence of ZsGreen was used to determine the relative number of viable cells. The error bars indicate the mean ± SD of triplicate experiments. $^{**}P < 0.01$ by the Student *t*-test.

To identify the mechanism that mediated the effects of platelets and supernatants of osteosarcoma-platelet reactants on osteosarcoma cell proliferation, we used arrays comprising a panel of antibodies specific for cytokines, growth factor receptors, or downstream signaling components. Incubation of the array with cell lysates prepared from reactants of MG63 cells and platelets increased the intensity of the spots corresponding to the positions of antibodies against phosphorylated PDGFRα, phosphorylated PDGFRβ, phosphorylated epidermal growth factor receptor (EGFR), and phosphorylated Akt1/2/3 antibodies (Figs. 2a–d). To exclude the possibility that the addition of platelets altered the respective protein expression levels in MG63 cells, we performed western blot analysis. Consistent with the array data, we confirmed the increase in phospho-PDGFRβ in MG63 cells that were co-cultured with platelets (Fig. 2e). Because PDGFRβ was not detected in the platelet lysate, indicating that co-culture induced PDGFRβ phosphorylation in MG63 cells. An increase in the level of phospho-Akt induced by co-culture was also detected using western blotting (Fig. 2e). Because the elecrophoretic mobility of mouse Akt in platelets appeared higher compared with human Akt in MG63 cells, the intensity of the phospho-Akt signal may represent phosphorylation of human but not mouse Akt. We obtained similar results using another HOS cell line (Fig. 2f). These data suggest that osteosarcoma-platelet interactions activate the PDGFR-Akt signaling pathway.

PDGFs released on the osteosarcoma cell-induced platelet aggregation contribute to the activation of the PDGFR-Akt signaling axis. Activation of PDGFRα and PDGFRβ is mediated by PDGFs, and only PDGF-BB can activate both PDGFRs. To determine whether PDGF-BB was released during the osteosarcoma cell-mediated platelet aggregation, we measured the amount of PDGF-BB in the supernatants of the osteosarcoma-platelet reactants using an enzyme linked immunosorbent assay (ELISA). The level of PDGF-BB was increased in supernatants of osteosarcoma-platelet aggregates compared with platelets alone (Fig. 3a). To assess the contribution of PDGFs to the activation of PDGFR-Akt axis, we treated MG63/ZsGreen and HOS/ZsGreen cells with the supernatant of the osteosarcoma-platelet reactant in the absence or presence of PDGFRs inhibitor, sunitinib. We found that the levels of phospho-PDGFRβ and phospho-Akt increased in osteosarcoma cell lines in the

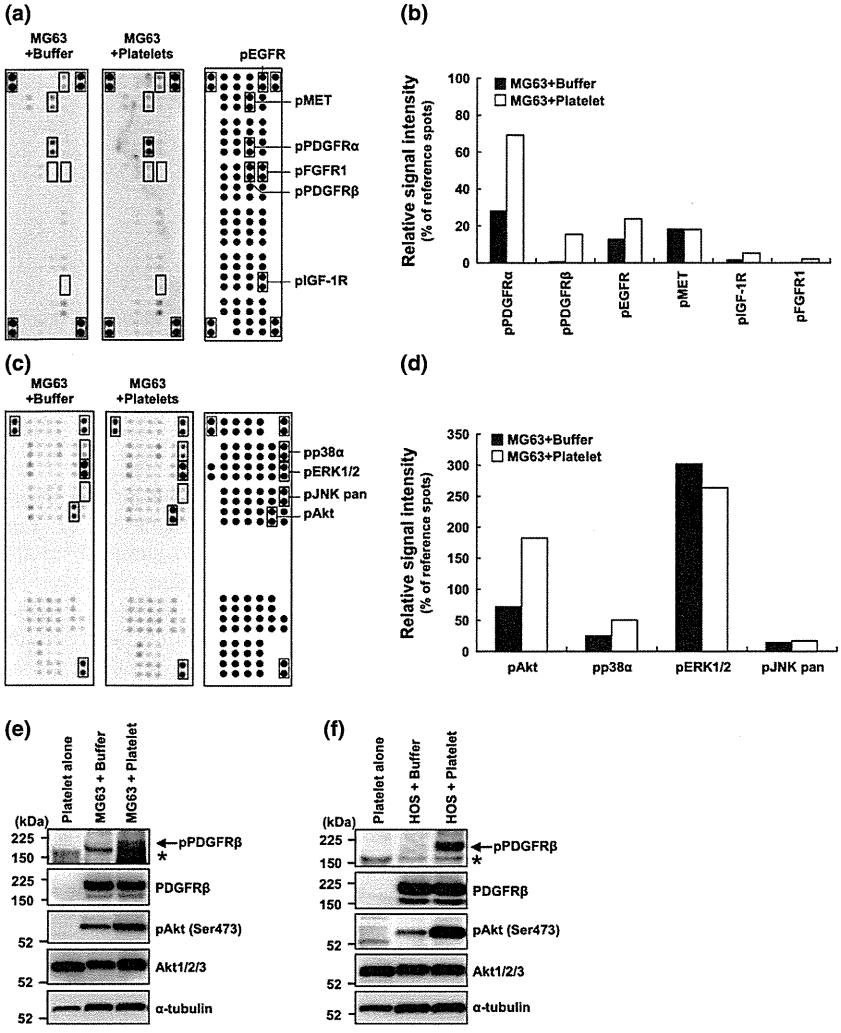

Fig. 2. Activation of the platelet derived growth factor receptor (PDGFR)-Akt signaling axis in MG63 cells co-cultured with platelets. (a, b) Platelets prepared with heparin from the whole blood of Jcl: ICR mice were resuspended in modified Tyrode's buffer containing 200 μM $CaCl_2$. MG63/ZsGreen cells were co-cultured with buffer alone (MG63 + Buffer) or platelets (MG63 + Platelet) for 2 h. The preparation of cell lysates and incubation with the human phospho-RTK array were performed according to the manufacturer's protocol. Representative images of the probed arrays are shown (a). The signal intensity of each spot was determined using an LAS-3000 mini and quantified using Multi Gauge ver.3.0 software. The signal intensities of eight reference spots (within red squares) in each membrane were measured and defined as 100%. The relative intensities of duplicate spots are shown (b). (c, d) Analysis of the human phospho-kinase array using lysates prepared from MG63 cells co-cultured with platelets in modified Tyrode's buffer containing 200 μM $CaCl_2$. MG63/ZsGreen cells were cultured with buffer alone (MG63 + Buffer) or with platelets (MG63 + Platelet) for 2 h. The preparation of cell lysates and incubation with the human phospho-kinase array were performed according to the manufacturer's protocol. Representative images of reacted membranes are shown (c). The signal intensity of each spot was measured using a LAS-3000 mini and quantified using Multi Gauge ver.3.0 software. The signal intensities of six reference spots (red squares) in each membrane were defined as 100%. The relative intensities of duplicate spots are shown (d). (e, f) Platelets prepared with 0.38% sodium citrate were resuspended Tyrode's buffer containing 200 μM $CaCl_2$. MG63/ZsGreen (e) or HOS/ZsGreen (f) cells were incubated with buffer alone or platelets (2.0×10^7/24-well) for 2 h. Platelets alone, osteosarcoma cells alone (+Buffer) or co-cultures of osteosarcoma cells with platelets (+Platelet) were lysed and immunoblotted using the antibodies to phospho-PDGFRβ, PDGFRβ, phospho-Akt (S473), Akt, or α-tubulin.

absence of, but not in the presence of sunitinib (Figs 3b,c). These results indicate that PDGFs released from activated platelets by the initiation of osteosarcoma-platelet interactions activated the PDGFR-Akt signaling axis.

Activation of the PDGFR-Akt signaling axis contributes to the platelet-dependent proliferation of osteosarcoma cell lines. To assess the role of the activation of the PDGFR-Akt axis in the growth of MG63 cells, we determined the effects of sunitinib, LY294002, or erlotinib, which inhibit the activity of the PDGFRs, phosphatidylinositol-4,5-bisphosphate 3-kinase (PI3K), or EGFR, respectively. Sunitinib and LY294002, but not erlotinib, inhibited the growth of MG63 and HOS cells when they were co-cultured with platelets (Figs 4a,b). These results indicate that activation of the PDGFR-Akt axis

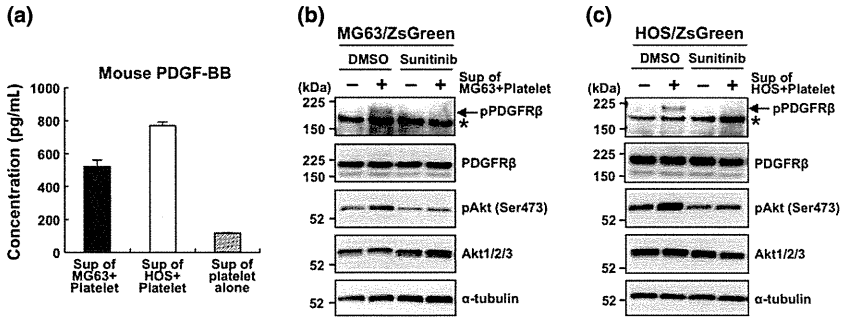

Fig. 3. Platelet-derived growth factors (PDGFs) released on the osteosarcoma-induced platelet aggregation contribute to the activation of the PDGFR-Akt signaling axis. (a–c) Washed mouse platelets (2.0×10^7 platelets) were resuspended in modified Tyrode's buffer containing 1% PPP and 200 μM $CaCl_2$ followed by incubation with PBS or with the indicated osteosarcoma cells (2.5×10^4 cells) for 30 min. After centrifuging twice at 10 000 *g* for 10 min, the concentration of PDGF-BB in the supernatants was measured using an enzyme linked immunosorbent assay (ELISA) (a). The cultured MG63/ZsGreen (b) and HOS/ZsGreen (c) cells were treated with (+) or without (–) the supernatant of osteosarcoma-platelet aggregates in the presence of DMSO or 1 μM sunitinib. After a 30-min incubation, cells were lysed with TENSV buffer and immunoblotted with the indicated antibodies.

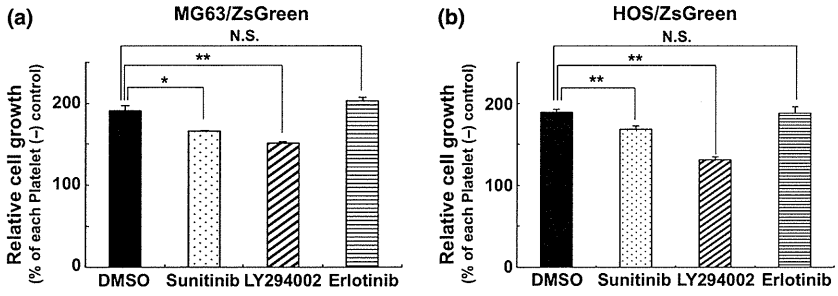

Fig. 4. Involvement of the platelet-derived growth factor receptor (PDGFR) -Akt signaling axis in the platelet-induced growth of osteosarcoma cells. (a, b) MG63/ZsGreen (a) or HOS/ZsGreen (b) cells in 24-well were co-cultured with platelets (2×10^7 in Tyrode's buffer containing 200 μM $CaCl_2$) in the presence of DMSO, the epidermal growth factor receptor (EGFR) inhibitor erlotinib (1 μM), the PDGFR inhibitor sunitinib (1 μM), or the PI3K inhibitor LY294002 (20 μM). After a 48-h incubation, cells were lysed and the fluorescence of ZsGreen was measured to determine relative cell growth. The error bars indicate the mean ± SD of triplicate experiments. $^{**}P < 0.01$ and $^{*}P < 0.05$ (Student's *t*-test). NS, not significant.

contributes to the platelet-dependent proliferation of osteosarcoma cells.

Discussion

Osteosarcoma is highly aggressive with distant metastasis, and approximately 20% of patients have metastases in lung or bone at diagnosis.[18] Although the frequency of 5-year disease-free survival of patients with nonmetastatic osteosarcoma is approximately 70%,[19] the average survival rate after recurrence in distant organs is only 1 year.[20] Therefore, metastasis is the most common cause of death of patients with osteosarcomas as well as other cancers. There is a positive correlation between the expression level of platelet aggregation-inducing factors and the potential of osteosarcomas to metastasize to the lung.[13] Mehta *et al.*[21] suggest that stimulation of platelets by osteosarcoma cells correlates with their potential to metastasize to the lung.

The platelet receptor glycoprotein Ibα, sialyl Lewis^x/sialyl Lewis^a, integrins, thrombospondin-1 (TSP-1), and Aggrus/podoplanin has been reported to induce platelet aggregation.[16,22–26] Among them, TSP-1 and Aggrus are key molecules that mediate osteosarcoma-induced platelet aggregation.[17,18] TSP-1 and Aggrus are expressed on cell surface, indicating that they may serve as targets of therapeutic antibodies against osteosarcoma. In fact, we confirmed Aggrus expression in the used two human osteosarcoma cell lines (Fig. S1a) and the addition of our established neutralizing anti-Aggrus antibody (MS-1)[14] suppressed the MG63-dependent platelet aggregation and the PDGF release from platelets at a significant level (Fig. S1b,c). These results suggest that Aggrus expression on osteosarcomas contributes to the interaction with platelets and that Aggrus could be a therapeutic target of osteosarcoma. We also observed the MG63-induced platelet aggregation was suppressed by the addition of antibody against von Willebrand factor, which is one of the platelet aggregation-mediating molecules and known to be overexpressed in metastatic osteosarcoma (Fig. S2).[13] Thus, von Willebrand factor also plays some roles in osteosarcoma-mediated platelet aggregation.

Platelet derived growth factor (PDGF) and the PDGFR are implicated in the pathogenesis of sarcomas such as Ewing sarcoma, chondrosarcoma, rhabdomyosarcoma, intimal sarcoma, and osteosarcoma.[27–30] Immunohistochemical analysis revealed that PDGFRα and PDGFRβ are frequently expressed in osteosarcomas (79.6% and 86%, respectively, $n = 54$), and the prognosis of patients with co-expression of PDGFRα and PDGF-AA is significantly poorer.[19] In the present study, osteosarcoma-platelet interactions promoted the proliferation of osteosarcoma cell lines through the activation of the PDGFR-Akt signaling axis (Fig. 2). However, sunitinib treatment partially suppressed the platelet-dependent proliferation of osteosarcoma cells (Fig. 4). Moreover, the inhibitory effects of a PI3K inhibitor LY294002, which functions downstream in the signaling pathways of certain receptor tyrosine kinases, were increased compared with sunitinib (Fig. 4). These results suggest the participation of other signaling pathways in the platelet-dependent proliferation of osteosarcoma cells. For example, insulin-like growth factor-1 (IGF-1), which is released from the α-granules of activated platelets, increases the growth of MG63 cells.[31] Although we did not detect other phosphorylated proteins, including the IGF-1 receptor, using antibody arrays, other proliferative signals may contribute to the platelet-dependent proliferation of osteosarcomas. Therefore, specific inhibitors that block osteosarcoma-platelet interactions may be useful for the suppression of platelet-dependent proliferation of osteosarcoma.

The use of chemotherapeutic agents is essential for the treatment of osteosarcoma patients; however, the efficacy of the current treatment regimen including adriamycin, which was originally developed in the mid-1980s, is limited.[19] Apoptosis induced by adriamycin was attenuated by co-culture with platelets in osteosarcomas (Fig. S3). Moreover, their invasiveness was promoted by co-culture with platelets (Fig. S4). Because prior administration of neutralizing anti-Aggrus antibodies has been reported to prevent hematogenous metastasis of Aggrus-positive tumor cells in mouse models [8,14,32] and to attenuate PDGF release from platelets (Fig. S1c), the combination therapy of anti-Aggrus antibodies with standard chemotherapeutic agents may be effective for inhibiting the proliferation of osteosarcomas and for preventing metastasis.

Acknowledgments

We thank Dr R. Katayama for valuable suggestions. This study was supported in part by the Advanced Research for Medical Products Mining Programme of the National Institute of Biomedical Innovation (NIBIO) (to NF), by a Grant-in-Aid for Scientific Research on Innovative Areas "Integrative Research on Cancer Microenvironment Network" from the Ministry of Education, Culture, Sports, Science, and Technology of Japan (to NF), and by a Grant-in-Aid for Young Scientists (B) (to ST).

Disclosure Statement

The authors have no conflict of interest.

References

1 Ritter J, Bielack SS. Osteosarcoma. *Ann Oncol* 2010; **21**(Suppl 7): vii320–5.
2 Kuijjer ML, Hogendoorn PC, Cleton-Jansen AM. Genome-wide analyses on high-grade osteosarcoma: making sense of a genomically most unstable tumor. *Int J Cancer* 2013; **133**: 2512–21.
3 Meyers PA, Heller G, Healey JH *et al.* Osteogenic sarcoma with clinically detectable metastasis at initial presentation. *J Clin Oncol* 1993; **11**: 449–53.
4 Bacci G, Briccoli A, Ferrari S *et al.* Neoadjuvant chemotherapy for osteosarcoma of the extremity: long-term results of the Rizzoli's 4th protocol. *Eur J Cancer* 2001; **37**: 2030–9.
5 Gay LJ, Felding-Habermann B. Contribution of platelets to tumour metastasis. *Nat Rev Cancer* 2011; **11**: 123–34.
6 Bambace NM, Holmes CE. The platelet contribution to cancer progression. *J Thromb Haemost* 2011; **9**: 237–49.
7 Sierko E, Wojtukiewicz MZ. Platelets and angiogenesis in malignancy. *Semin Thromb Hemost* 2004; **30**: 95–108.
8 Fujita N, Takagi S. The impact of Aggrus/podoplanin on platelet aggregation and tumour metastasis. *J Biochem* 2012; **152**: 407–13.
9 Schumacher D, Strilic B, Sivaraj KK, Wettschureck N, Offermanns S. Platelet-derived nucleotides promote tumor-cell transendothelial migration and metastasis via P2Y receptor. *Cancer Cell* 2013; **24**: 130–7.
10 Gasic GJ, Gasic TB, Stewart CC. Antimetastatic effects associated with platelet reduction. *Proc Natl Acad Sci USA* 1968; **1**: 46–52.
11 Karpatkin S, Pearlstein E, Salk PL, Yogeeswaran G. Role of platelets in tumor cell metastasis. *Ann N Y Acad Sci* 1981; **370**: 101–18.
12 Kunita A, Kashima TG, Morishita Y *et al.* The platelet aggregation-inducing factor aggrus/podoplanin promotes pulmonary metastasis. *Am J Pathol* 2007; **170**: 1337–47.
13 Eppert K, Wunder JS, Aneliunas V, Kandel R, Andrulis IL. von Willebrand factor expression in osteosarcoma metastasis. *Mod Pathol* 2005; **18**: 388–97.
14 Takagi S, Sato S, Oh-Hara T *et al.* Platelets promote tumor growth and metastasis via direct interaction between Aggrus/podoplanin and CLEC-2. *PLoS ONE* 2013; **8**: e73609.
15 Nakazawa Y, Takagi S, Sato S *et al.* Prevention of hematogenous metastasis by neutralizing mice and its chimeric anti-Aggrus/podoplanin antibodies. *Cancer Sci* 2011; **102**: 2051–7.
16 Clezardin P, Serre CM, Trzeciak MC, Drouin J, Delmas PD. Thrombospondin binds to the surface of human osteosarcoma cells and mediates platelet-osteosarcoma cell interaction. *Cancer Res* 1991; **51**: 2621–7.
17 Kunita A, Kashima TG, Ohazama A, Grigoriadis AE, Fukayama M. Podoplanin is regulated by AP-1 and promotes platelet aggregation and cell migration in osteosarcoma. *Am J Pathol* 2011; **179**: 1041–9.
18 Voland C, Serre CM, Delmas P, Clézardin P. Platelet-osteosarcoma cell interaction is mediated through a specific fibrinogen-binding sequence located within the N-terminal domain of thrombospondin 1. *J Bone Miner Res* 2000; **15**: 361–8.
19 Kubo T, Piperdi S, Rosenblum J *et al.* Platelet-derived growth factor receptor as a prognostic marker and a therapeutic target for imatinib mesylate therapy in osteosarcoma. *Cancer* 2008; **112**: 2119–29.
20 Kempf-Bielack B, Bielack SS, Jürgens H *et al.* Osteosarcoma relapse after combined modality therapy: an analysis of unselected patients in the Cooperative Osteosarcoma Study Group (COSS). *J Clin Oncol* 2005; **23**: 559–68.
21 Mehta P, Lawson D, Ward MB, Kimura A, Gee A. Effect of human tumor cells on platelet aggregation: potential relevance to pattern of metast. *Cancer Res* 1987; **47**: 3115–7.
22 Oleksowicz L, Mrowiec Z, Schwartz E, Khorshidi M, Dutcher JP, Puszkin E. Characterization of tumor-induced platelet aggregation: the role of immunorelated GPIb and GPIIb/IIIa expression by MCF-7 breast cancer cells. *Thromb Res* 1995; **79**: 261–74.
23 Nakamori S, Kameyama M, Imaoka S *et al.* Increased expression of sialyl Lewis^x antigen correlates with poor survival in patients with colorectal carcinoma: clinicopathological and immunohistochemical study. *Cancer Res* 1993; **53**: 3632–7.
24 Mannori G, Crottet P, Cecconi O *et al.* Differential colon cancer cell adhesion to E-, P-, and L-selectin: role of mucin-type glycoproteins. *Cancer Res* 1995; **55**: 4425–31.
25 Felding-Habermann B, Habermann R, Saldívar E, Ruggeri ZM. Role of beta3 integrins in melanoma cell adhesion to activated platelets under flow. *J Biol Chem* 1996; **271**: 5892–900.
26 Kato Y, Fujita N, Kunita A *et al.* Molecular identification of Aggrus /T1alpha as a platelet aggregation-inducing factor expressed in colorectal tumors. *J Biol Chem* 2003; **278**: 51599–605.
27 Uren A, Merchant MS, Sun CJ *et al.* Beta-platelet-derived growth factor receptor mediates motility and growth of Ewing's sarcoma cells. *Oncogene* 2003; **22**: 2334–42.
28 Sulzbacher I, Birner P, Trieb K, Mühlbauer M, Lang S, Chott A. Platelet-derived growth factor-alpha receptor expression supports the growth of conventional chondrosarcoma and is associated with adverse outcome. *Am J Surg Pathol* 2001; **25**: 1520–7.
29 McDermott U, Ames RY, Iafrate AJ *et al.* Ligand-dependent platelet-derived growth factor receptor (PDGFR)-alpha activation sensitizes rare lung cancer and sarcoma cells to PDGFR kinase inhibitors. *Cancer Res* 2009; **69**: 3937–46.
30 Dewaele B, Floris G, Finalet-Ferreiro J *et al.* Coactivated platelet-derived growth factor receptor α and epidermal growth factor receptor are potential therapeutic targets in intimal sarcoma. *Cancer Res* 2010; **70**: 7304–14.
31 Raile K, Hille R, Laue S *et al.* Insulin-like growth factor I (IGF-I) stimulates proliferation but also increases caspase-3 activity, Annexin-V binding, and DNA-fragmentation in human MG63 osteosarcoma cells: co-activation of pro- and anti-apoptotic pathways by IGF-I. *Horm Metab Res* 2003; **35**: 786–93.
32 Takagi S, Oh-Hara T, Sato S, Gong B, Takami M, Fujita N. Expression of Aggrus/podoplanin in bladder cancer and its role in pulmonary metastasis. *Int J Cancer* 2014; **134**: 2605–14.

Supporting Information

Additional supporting information may be found in the online version of this article:

Fig. S1. Involvement of Aggrus/podoplanin in platelet aggregation and PDGF release during osteosarcoma cell-induced platelet aggregation.

Fig. S2. Attenuation of MG63-dependent platelet aggregation by an anti-von Willebrand factor (vWF) antibody.

Fig. S3. Co-culture with platelets contributes to the resistance to apoptosis induced by adriamycin in osteosarcoma cells.

Fig. S4. Platelets promote invasiveness of osteosarcomas.

Published OnlineFirst March 27, 2014; DOI: 10.1158/2159-8290.CD-13-0846

RESEARCH ARTICLE

The ALK Inhibitor Ceritinib Overcomes Crizotinib Resistance in Non-Small Cell Lung Cancer

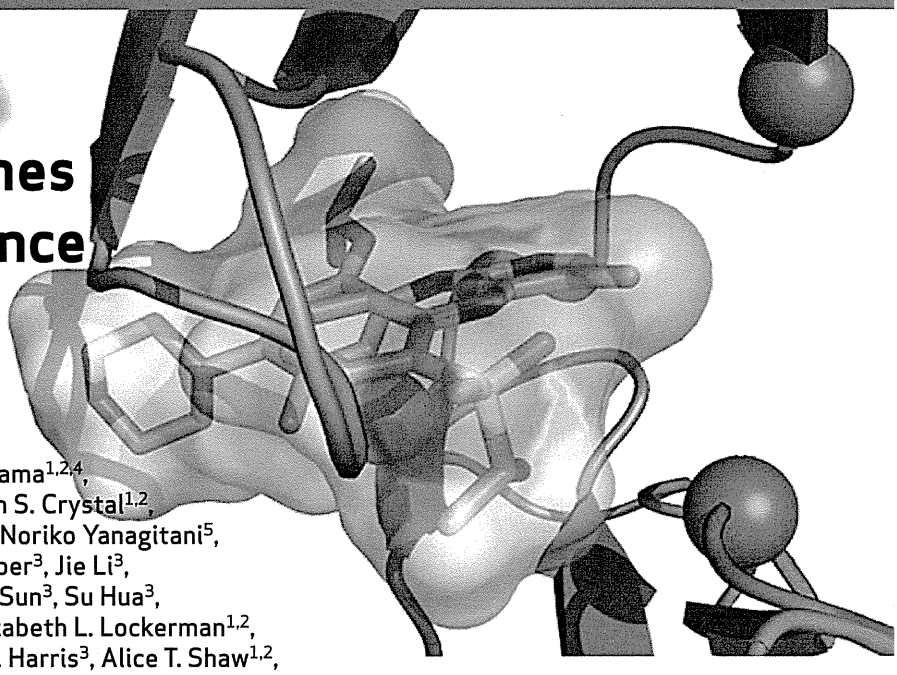

Luc Friboulet[1,2], Nanxin Li[3], Ryohei Katayama[1,2,4], Christian C. Lee[3], Justin F. Gainor[1,2], Adam S. Crystal[1,2], Pierre-Yves Michellys[3], Mark M. Awad[1,2], Noriko Yanagitani[5], Sungjoon Kim[3], AnneMarie C. Pferdekamper[3], Jie Li[3], Shailaja Kasibhatla[3], Frank Sun[3], Xiuying Sun[3], Su Hua[3], Peter McNamara[3], Sidra Mahmood[1,2], Elizabeth L. Lockerman[1,2], Naoya Fujita[4], Makoto Nishio[5], Jennifer L. Harris[3], Alice T. Shaw[1,2], and Jeffrey A. Engelman[1,2]

ABSTRACT

Non–small cell lung cancers (NSCLC) harboring anaplastic lymphoma kinase (*ALK*) gene rearrangements invariably develop resistance to the ALK tyrosine kinase inhibitor (TKI) crizotinib. Herein, we report the first preclinical evaluation of the next-generation ALK TKI, ceritinib (LDK378), in the setting of crizotinib resistance. An interrogation of *in vitro* and *in vivo* models of acquired resistance to crizotinib, including cell lines established from biopsies of patients with crizotinib-resistant NSCLC, revealed that ceritinib potently overcomes crizotinib-resistant mutations. In particular, ceritinib effectively inhibits ALK harboring L1196M, G1269A, I1171T, and S1206Y mutations, and a cocrystal structure of ceritinib bound to ALK provides structural bases for this increased potency. However, we observed that ceritinib did not overcome two crizotinib-resistant ALK mutations, G1202R and F1174C, and one of these mutations was identified in 5 of 11 biopsies from patients with acquired resistance to ceritinib. Altogether, our results demonstrate that ceritinib can overcome crizotinib resistance, consistent with clinical data showing marked efficacy of ceritinib in patients with crizotinib-resistant disease.

SIGNIFICANCE: The second-generation ALK inhibitor ceritinib can overcome several crizotinib-resistant mutations and is potent against several *in vitro* and *in vivo* laboratory models of acquired resistance to crizotinib. These findings provide the molecular basis for the marked clinical activity of ceritinib in patients with *ALK*-positive NSCLC with crizotinib-resistant disease. *Cancer Discov; 4(6); 662–73. ©2014 AACR.*

See related commentary by Ramalingam and Khuri, p. 634.

Authors' Affiliations: [1]Massachusetts General Hospital Cancer Center; [2]Department of Medicine, Harvard Medical School, Boston, Massachusetts; [3]Genomics Institute of the Novartis Research Foundation, San Diego, California; [4]Cancer Chemotherapy Center and [5]Cancer Institute Hospital, Japanese Foundation for Cancer Research, Tokyo, Japan

Note: Supplementary data for this article are available at Cancer Discovery Online (http://cancerdiscovery.aacrjournals.org/).

L. Friboulet, N. Li, and R. Katayama contributed equally to this work.

Corresponding Authors: Jeffrey A. Engelman, Massachusetts General Hospital Cancer Center, CNY 149, 13th Street, Charlestown, MA 02129. Phone: 617-724-7298; Fax: 617-724-9648; E-mail: jengelman@partners.org; Alice T. Shaw, ashaw1@mgh.harvard.edu; and Jennifer L. Harris, jharris@gnf.org.

doi: 10.1158/2159-8290.CD-13-0846

Published OnlineFirst March 27, 2014; DOI: 10.1158/2159-8290.CD-13-0846

INTRODUCTION

Chromosomal rearrangements of anaplastic lymphoma kinase (*ALK*) are detected in 3% to 7% of non–small cell lung cancers (NSCLC; refs. 1, 2). These rearrangements result in constitutively active ALK fusion proteins with potent transforming activity (2, 3). Lung cancers with *ALK* rearrangements are highly sensitive to ALK tyrosine kinase inhibition, underscoring the notion that such cancers are addicted to ALK kinase activity. On the basis of early-phase studies, the multitargeted tyrosine kinase inhibitor (TKI) crizotinib was approved by the FDA in 2011 to treat patients with advanced NSCLC harboring *ALK* rearrangements (1). However, despite a high response rate of 60% in *ALK*-rearranged NSCLC, most patients develop resistance to crizotinib, typically within 1 to 2 years.

Studies of *ALK*-rearranged lung cancers with acquired resistance to crizotinib have identified *ALK* fusion gene amplification and secondary ALK tyrosine kinase (TK) domain mutations in about one third of cases (4–6). To date, seven different acquired resistance mutations have been identified among crizotinib-resistant patients. The most frequently identified secondary mutations are L1196M and G1269A. In addition to these mutations, the 1151T-ins, L1152R, C1156Y, G1202R, and S1206Y mutations have also been detected in crizotinib-resistant cancers (4, 6–10). In approximately one third of crizotinib-resistant tumors, there is evidence of activation of bypass signaling tracts such as EGFR or c-KIT (6, 9). In the remaining one third of crizotinib-resistant tumors, the resistance mechanisms remain to be identified.

Next-generation ALK inhibitors with improved potency and selectivity compared with crizotinib have been developed to overcome crizotinib resistance in the clinic. We previously evaluated the ability of several ALK TKIs (TAE684, AP26113, ASP3026, and CH5424802) to inhibit ALK activity in models harboring different *ALK* secondary mutations (6, 11). These studies revealed variable sensitivity to these ALK inhibitors depending on the specific resistance mutation present. For example, the gatekeeper L1196M mutation was sensitive to TAE684, AP26113, and ASP3026, whereas 1151T-ins conferred resistance to all next-generation ALK TKIs. Ceritinib is an ATP-competitive, potent, and selective next-generation ALK inhibitor (12). The kinase selectivity has been tested in a cellular proliferation assay against 16 different kinases, and aside from ALK, no inhibition below 100 nmol/L was observed (12). In the phase I study of ceritinib in *ALK*-positive NSCLC, marked antitumor activity has been observed in both crizotinib-relapsed and crizotinib-naïve patients (13, 14). On the basis of this impressive clinical activity, ceritinib received FDA approval on April 29, 2014.

Herein, we present the first report examining the activity of ceritinib in preclinical models of *ALK*-positive lung cancer with acquired resistance to crizotinib, as well as an early biologic insight into mechanisms of resistance to ceritinib arising in patients.

Table 1. Ceritinib is a potent ALK inhibitor

	GI_{50} (nmol/L)		
	Crizotinib	Ceritinib	Fold
ALK enzymatic assay	3	0.15	20
H2228	107	3.8	28
H3122	245	6.3	39

NOTE: GI_{50} values for *in vitro* ALK enzymatic assay or H3122 and H2228 cell survival assay for crizotinib and ceritinib are shown.

RESULTS

Ceritinib Exhibits Potent Activity in Crizotinib-Naïve *ALK*-Positive NSCLC Models

In vitro enzymatic studies revealed that ceritinib was approximately 20-fold more potent against ALK than crizotinib (Table 1). Similarly, ceritinib was more potent than crizotinib against two *ALK*-rearranged lung cancer cell lines, H3122 and H2228 (Fig. 1A and B, Table 1). Accordingly, ceritinib led to suppression of ALK phosphorylation as well as the downstream PI3K–AKT, MEK–ERK, and mTOR signaling pathways at lower doses than crizotinib (Fig. 1C and D).

To further assess the cellular specificity of ceritinib, we determined the GI_{50} (concentration needed to reduce the growth of treated cells to half that of untreated cells) of ceritinib against a panel of tumor cell lines bearing different oncogenic drivers. Whereas ceritinib was potent against the two lung cancer cell lines with *ALK* rearrangements, it was not potent against NSCLC or breast cancer cell lines driven by KRAS, EGFR, PI3K, or HER2, with GI_{50}s >1 μmol/L (Supplementary Fig. S1A).

We next compared the efficacy of ceritinib and crizotinib *in vivo* using treatment-naïve H2228 xenograft models (Fig. 1E). Tumor-bearing animals were treated with either high-dose crizotinib (100 mg/kg) or ceritinib (25 mg/kg or 50 mg/kg) once daily for 14 days. Both crizotinib (100 mg/kg) and ceritinib (25 and 50 mg/kg) were well tolerated in this study (Supplementary Fig. S1B). As expected, marked tumor regression was observed in all groups during the treatment. After treatment was stopped, the animals were monitored for tumor progression. Although recurrent tumors were detected within 11 days of drug withdrawal in mice treated with crizotinib, mice treated with ceritinib at 50 mg/kg remained in complete remission with no discernible tumor growth for 4 months. In the mice treated with ceritinib at 25 mg/kg, tumor regrowth was observed in 4 of 8 animals after 1 month, whereas complete remission was maintained in the other 4 animals for 4 months. Thus, ceritinib had more durable antitumor activity than crizotinib, even after the drugs were discontinued. It is also worth noting that the exposure of crizotinib at 100 mg/kg is approximately 3-fold to 5-fold greater than the exposures achieved at the human maximum tolerated dose (MTD; 250 mg, twice a day; ref. 15) and that ceritinib at 25 to 50 mg/kg is predicted to be achievable at

Published OnlineFirst March 27, 2014; DOI: 10.1158/2159-8290.CD-13-0846

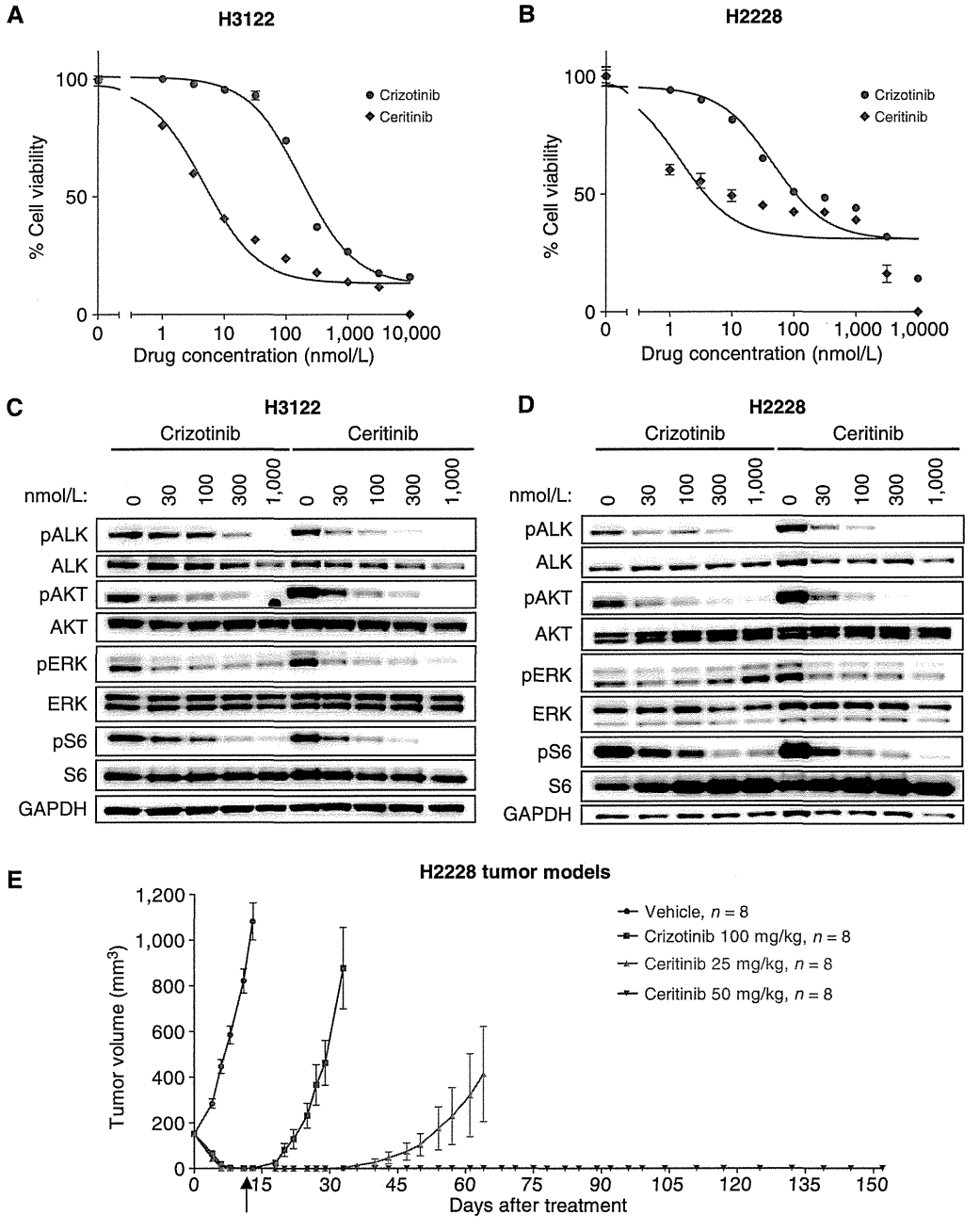

Figure 1. Ceritinib is a potent ALK inhibitor in crizotinib-naïve models. **A** and **B,** cell survival assay of H3122 (**A**) and H2228 (**B**) cells treated with the indicated doses of crizotinib or ceritinib for 72 hours. Cell survival was assayed by CellTiter-Glo. **C** and **D,** H3122 (**C**) and H2228 (**D**) cells were treated with the indicated concentrations of crizotinib or ceritinib for 6 hours. Lysates were probed with antibodies directed against the specified proteins. **E,** SCID beige bearing H2228 cells were administered crizotinib or ceritinib orally once daily for 14 days. The arrow indicates when treatments were stopped, and tumor growth was monitored in animals up to 4 months. Tumor volumes, mean ± SD ($n = 8$). p, phosphorylated.

the human MTD (750 mg every day). We also evaluated the efficacy of ceritinib in a primary explant model derived from a crizotinib-naïve NSCLC tumor MGH006 (6). Treatment of these mice with 25 mg/kg ceritinib also led to tumor regressions (Supplementary Fig. S1C). Altogether, these data demonstrate that ceritinib is potent against crizotinib-naïve *ALK*-rearranged cell lines and tumor models *in vivo* and *in vitro*.

Ceritinib Is Active against Patient-Derived Cell Lines from Crizotinib-Resistant Cancers with and without Resistant Mutations

To investigate the activity of ceritinib against crizotinib-resistant mutations, we used crizotinib-resistant cell line models harboring the two most common EML4–ALK

Published OnlineFirst March 27, 2014; DOI: 10.1158/2159-8290.CD-13-0846

A

Cell line	ALK mutation	GI_{50} (nmol/L) Crizotinib	GI_{50} (nmol/L) Ceritinib	Fold
H3122 CR1	L1196M	2884	230	13
MGH021-4	G1269A	500	80	6
MGH045	L1196M	891	25	36

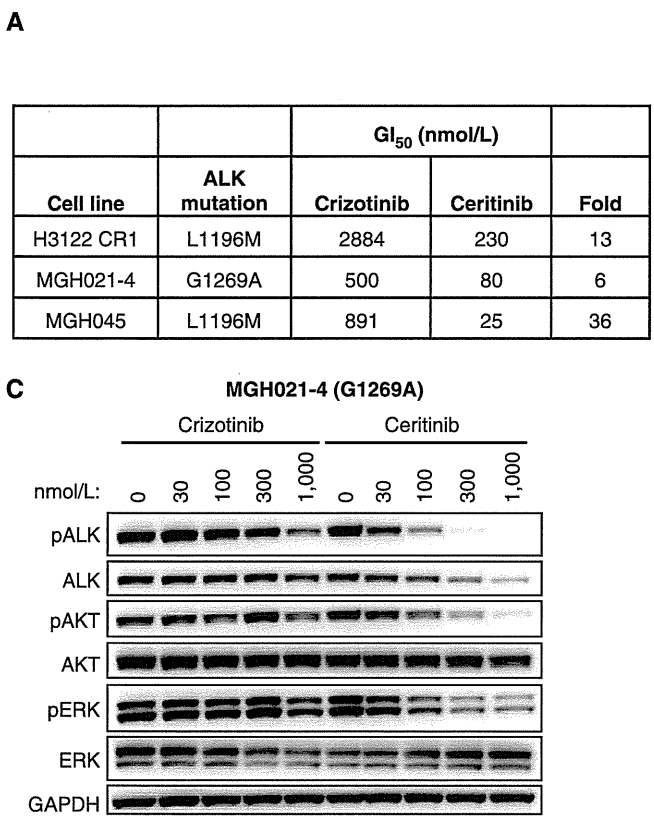

Figure 2. EML4-ALK L1196M and G1269A mutations are sensitive to ceritinib *in vitro*. **A,** GI_{50} values of cell survival assay for crizotinib or ceritinib in cell lines harboring L1196M or G1269A crizotinib resistant mutations. **B** to **D,** H3122 CR1 (**B**), MGH021-4 (**C**), and MGH045 (**D**) cells were treated with the indicated concentrations of crizotinib or ceritinib for 6 hours. Lysates were probed with antibodies directed against the indicated proteins. **E,** nude mice bearing the MGH045 cell line were treated with 100 mg/kg crizotinib or ceritinib 25 mg/kg. Tumor volumes, mean ± SD ($n = 6$). p, phosphorylated.

mutations, L1196M and G1269A. We have previously described the H3122 CR1 crizotinib-resistant cell line, which developed resistance *in vitro* by chronic exposure to crizotinib. This cell line harbors both the L1196M *EML4–ALK* gatekeeper mutation and amplification of the *EML4–ALK* allele (11). In addition, we also examined two novel cell lines established from biopsies of patients whose *ALK*-rearranged lung cancers had become resistant to crizotinib in the clinic. These two patient-derived resistant lines, MGH045 and MGH021-4, harbor the L1196M and G1269A mutations, respectively. The MGH021-4 line is a clonal cell line established from MGH021, a tumor harboring both 1151T-ins and G1269A mutations; MGH021-4 cells harbor only the G1269A mutation (5). This clone, therefore, represents an early generation of the patient-derived cell line. The GI_{50} values of ceritinib against all of these resistant cell lines were decreased 6-fold to 36-fold compared with crizotinib (Fig. 2A and Supplementary Fig. S2A–S2C). Accordingly, phosphorylation of ALK and downstream ERK and AKT were more effectively suppressed by lower doses of ceritinib compared with crizotinib (Fig. 2B–D).

To further assess the activity of ceritinib against crizotinib-resistant *ALK*-positive tumors *in vivo*, we examined the efficacy of ceritinib against xenografts derived from MGH045 cells that harbor the L1196M resistance mutation. As shown in Fig. 2E, treatment of MGH045 tumor-bearing mice with

Published OnlineFirst March 27, 2014; DOI: 10.1158/2159-8290.CD-13-0846

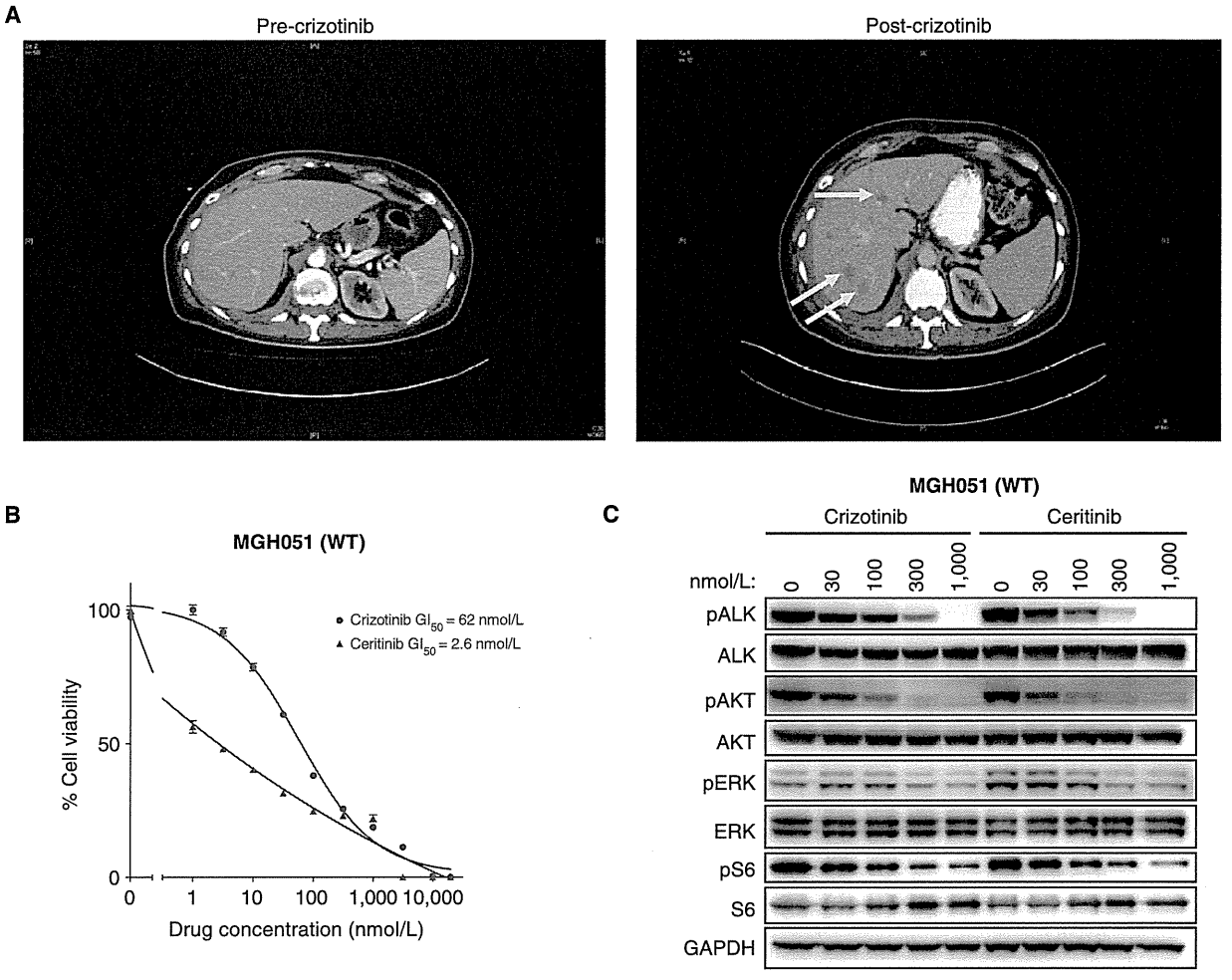

Figure 3. Ceritinib is active in ALK wild-type (WT) crizotinib-resistant cell line. **A,** abdominal computed tomography (CT) images of patient MGH051 before treatment with crizotinib and after 11 weeks of crizotinib. Several new hepatic metastases (yellow arrows) were detectable after crizotinib treatment consistent with disease progression. A repeat biopsy of a hepatic metastasis was performed within 2 weeks of crizotinib discontinuation. **B,** MGH051 cells were treated with the indicated doses of crizotinib or ceritinib for 7 days. After the incubation, the cell survival was assayed by CellTiter-Glo. **C,** MGH051 cells were treated with the indicated concentrations of crizotinib or ceritinib for 24 hours. Lysates were probed with antibodies directed against the indicated proteins.

low-dose ceritinib (25 mg/kg) was more effective than with high-dose crizotinib in controlling tumor growth. These data demonstrate that ceritinib is active against cancers derived from patients with acquired resistance to crizotinib and is more potent than crizotinib against *ALK*-rearranged cancers harboring the L1196M and G1269A resistance mutations.

The ongoing clinical trial of ceritinib demonstrates that crizotinib-resistant *ALK*-positive tumors, including tumors without *ALK* mutation or gene amplification, are responsive to ceritinib treatment (13). This raises the possibility that many of these resistant tumors may develop because of inadequate target suppression. We investigated the efficacy of crizotinib and ceritinib against a crizotinib-resistant *ALK*-positive cell line without *ALK* resistance mutations, MGH051. As shown in Fig. 3A, this cell line was derived from a biopsy of a liver lesion that developed in a patient on crizotinib. Assessment of the biopsy sample revealed no *ALK* mutations or gene amplification. The cell line derived from the biopsy also did not harbor any *ALK* resistance mutations. This resistant cell line was highly sensitive to ceritinib *in vitro*, and, surprisingly, the MGH051 cell line was also sensitive to crizotinib (Fig. 3B). Accordingly, phosphorylation of ALK and downstream AKT and ERK was efficiently suppressed by crizotinib and ceritinib (Fig. 3C). These data suggest that cancers with acquired resistance to crizotinib without *ALK*-resistant mutations may remain sensitive to ALK inhibition (please see "Discussion").

Assessment of Ceritinib Activity against a Panel of *ALK* Mutations

To systematically assess the potency of ceritinib against *ALK* resistance mutations, we used Ba/F3 cells engineered

Published OnlineFirst March 27, 2014; DOI: 10.1158/2159-8290.CD-13-0846

to express wild-type *EML4–ALK* or one of the nine different resistance mutations. In this system, ceritinib was approximately 10-fold more potent against wild-type *EML4–ALK* than crizotinib. Whereas all these secondary mutations induced crizotinib resistance, ceritinib was potent in inhibiting the growth of Ba/F3 cells expressing four of the resistance mutations, including L1196M, G1269A, S1206Y, and I1171T (Fig. 4A; Supplementary Fig. S3; Supplementary Table S1). However, C1156Y, G1202R, 1151T-ins, L1152R, and F1174C mutations also conferred resistance to ceritinib, although ceritinib was still more potent than crizotinib against these mutations. Thus, the most common crizotinib-resistant mutations were substantially more sensitive to ceritinib than crizotinib, whereas less common resistance mutations conferred resistance to both crizotinib and ceritinib.

Structural Basis for Increased Potency of Ceritinib against *ALK* Crizotinib-Resistant Mutations

To glean insights into the structural basis for the ability of ceritinib to maintain activity toward select crizotinib-resistant mutants, the structure of the ALK catalytic domain complexed with ceritinib was determined (Fig. 4B; PDB 4MKC) and compared with the structure of the ALK catalytic domain bound to crizotinib (Fig. 4C; PDB 2XP2; ref. 16). As shown in Fig. 4A, ceritinib retains potency toward the most common G1269A and L1196M crizotinib-resistant mutants. The cocrystal structure reveals that G1269 is situated just proximal to D1270 of the activation loop DFG-motif. Although mutation to Ala in the G1269A mutant would not be predicted to present any steric obstruction to ceritinib binding, it would be predicted to introduce a steric clash to crizotinib binding due to the proximity of the phenyl ring of crizotinib. The Cl moiety of the pyrimidine hinge-binding core of ceritinib is juxtaposed with the L1196 side chain and participates in a hydrophobic interaction with the Leu side chain. In the L1196M mutant, the Cl moiety of ceritinib can interact with Met, which may compensate for the loss of interaction between Cl and the Leu side chain in wild-type ALK. In contrast, introduction of a Met at the gatekeeper position 1196 likely adversely affects crizotinib binding through both steric interference and unfavorable interactions with the 2-amino substituent of the pyridinyl hinge-binding core and the methyl substituent of the alkoxy moiety of crizotinib. These structural findings are in agreement with the increased potency of ceritinib versus crizotinib against these resistance mutations.

In contrast with G1269A and L1196M mutations, ceritinib is not potent against the G1202R crizotinib-resistant mutation (Fig. 4A). The crystal structure reveals that mutation of G1202 to a larger, bulky, and charged side chain would be incompatible with ceritinib or crizotinib ALK binding due to steric hindrance (6). This steric obstruction leads to a loss in potency as reflected by the shift in IC_{50} values observed for ceritinib and crizotinib. In contrast with the G1202R mutation, the T1151 insertion, L1152P, C1156Y, and F1174C inhibitor–resistant mutants all map to the N-terminal lobe of the ALK catalytic domain and flank opposing ends of the αC-helix. The locations of these mutants do not directly contribute to inhibitor binding in cocrystal structures. Interestingly, positions T1151 and F1174 in ALK have been previously identified as sites of activating gain-of-function mutations in neuroblastoma (17). Although difficult to predict without structural and biochemical analyses of these mutants, T1151 is adjacent to the catalytically important K1150, and insertion at this position, along with the F1174C, L1152P, and C1156Y inhibitor-resistant mutants, likely influences αC-helix mobility and conformational dynamics of the catalytic domain. Previously reported structures of nonphosphorylated ALK in the apo, ADP, and inhibitor-bound forms suggest the ALK catalytic domain structure possesses a "DFG-in" conformation (18) with a unique activation loop conformation. It is conceivable that these mutations destabilize the ALK conformation and shift the conformational equilibrium toward those that are no longer able to bind the inhibitor. It is also possible that these mutations could decrease the K_m for ATP, rendering ceritinib/crizotinib a less effective ATP competitive inhibitor.

Crizotinib-Resistant Tumors Harboring EML4-ALK Wild-Type, I1171T, or C1156Y Mutations Are Sensitive to Ceritinib *In Vivo*

To evaluate the activity of ceritinib against crizotinib-resistant tumors *in vivo*, crizotinib-resistant H2228 xenograft tumors were generated by treatment with escalating doses of crizotinib (from 50 to 100 mg/kg). Tumors that progressed during treatment with 100 mg/kg crizotinib were analyzed for resistance mechanisms. Typical tumor responses and resistance are shown for 3 animals in Supplementary Fig. S4, and are representative of the 80 animals used in this study. To determine mechanisms of resistance to crizotinib, we sequenced the ALK kinase domain of all 80 tumors and identified three distinct resistance mutations in six tumors. The G1202R, C1156Y, and I1171T mutations were detected in three, two, and one resistant tumors, respectively. Of these three mutations, G1202R and C1156Y have been previously reported in patients with NSCLC who relapsed on crizotinib (6, 7). Interestingly, I1171T has not yet been reported from crizotinib-resistant patients but was identified in an *in vitro* mutagenesis screen for resistance mutations (19).

The efficacy of ceritinib was tested against these crizotinib-resistant H2228 xenograft tumor models as well as one of the resistance models that did not harbor a resistance mutation nor *ALK* amplification (data not shown). Although each was resistant to crizotinib at 100 mg/kg, ceritinib suppressed tumor growth in multiple resistance models (Fig. 5A–D). In the wild-type and I1171T resistant models, ceritinib demonstrated impressive antitumor activity, whereas it was less active in the C1156Y-resistant model and was inactive against the G1202R-resistant model. These data are consistent with the Ba/F3 models in which ceritinib was more potent against I1171T than the C1156Y and G1202R mutants (Fig. 4A). The studies shown herein provide evidence that ceritinib can overcome resistance *in vivo*, especially in tumors harboring wild-type, L1196M, or I1171T ALK fusions at a dose that is predicted to be achievable in humans. Of note, it is rather interesting that ceritinib overcame crizotinib resistance in the

Published OnlineFirst March 27, 2014; DOI: 10.1158/2159-8290.CD-13-0846

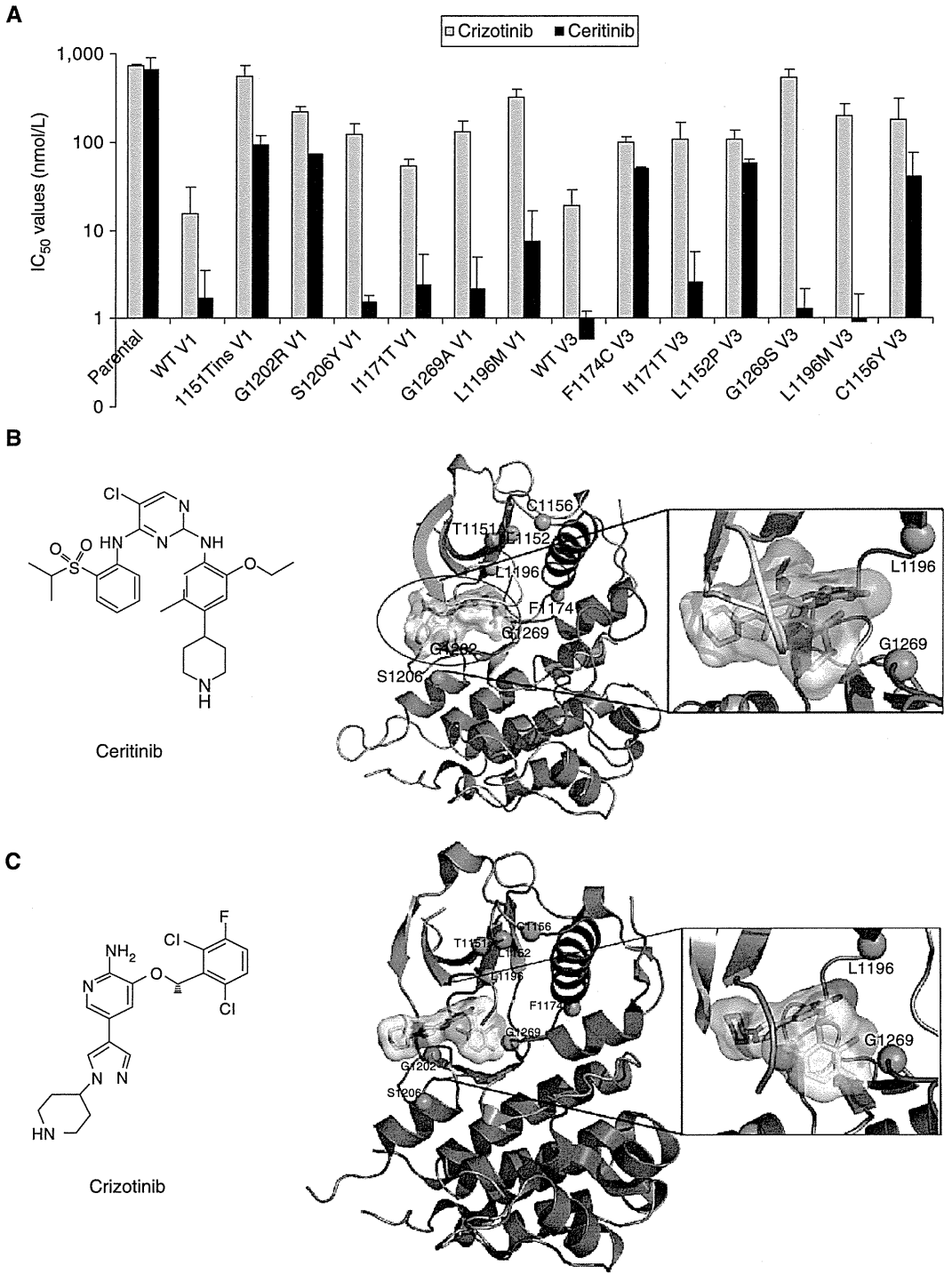

Figure 4. Ba/F3 models of ALK-crizotinib–resistant mutations. **A,** IC_{50} of ceritinib across different Ba/F3 cell lines expressing wild-type or mutated *ALK* TK and including parental, IL3-dependent Ba/F3 cells are shown. **B** and **C,** ALK-resistant mutations mapped onto ALK/ceritinib (PDB 4MKC; **B**) and ALK/crizotinib (PDB 2XP2; **C**) cocrystal structures. β-Strand secondary structural elements of the N-terminal lobe and the αC-helix of the N-terminal lobe are shown in orange and purple, respectively. Helical structural elements of the C-terminal lobe are shown in blue. Residues of the activation loop (A-loop) and catalytic loop are shown in red and orange, respectively. Residues involved in resistant mutations are depicted as green spheres. Inhibitor molecules are depicted as stick representations with carbons colored yellow and cyan for crizotinib and ceritinib, respectively. Nitrogen is colored dark blue, oxygen is colored red, and chlorine green for both inhibitors. Fluoride is colored white (crizotinib) and sulfur atoms are colored yellow (ceritinib). Transparent surfaces for the inhibitors are displayed. Zoomed-in view boxes for G1269 and L1196 residues are shown. Figures were rendered with MacPymol (The PyMOL Molecular Graphics System, Version 1.4 Schrödinger, LLC).

Published OnlineFirst March 27, 2014; DOI: 10.1158/2159-8290.CD-13-0846

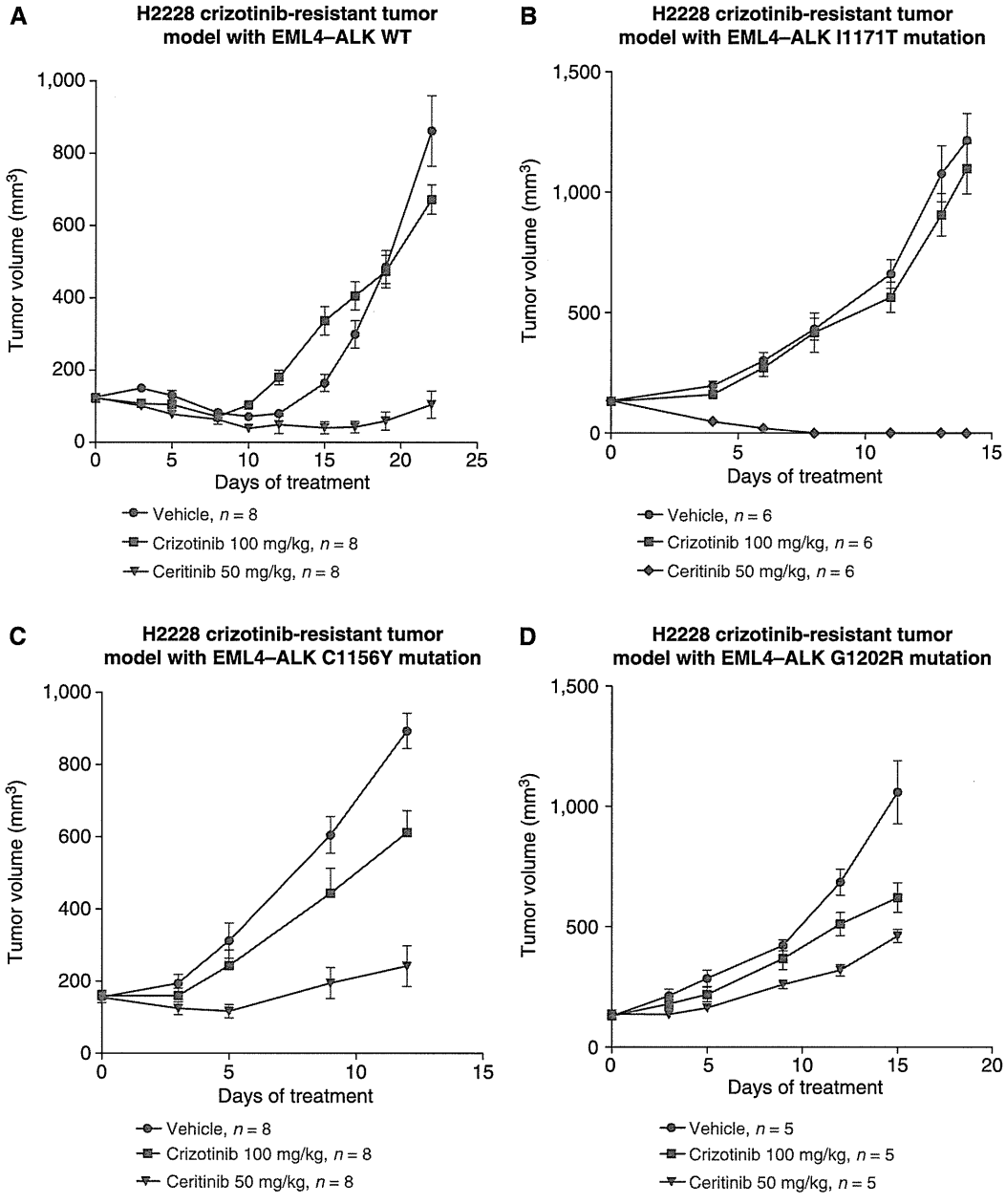

Figure 5. EML4-ALK C1156Y, I1171T, G1202R mutations' sensitivity to ceritinib. **A** to **D**, SCID beige mice bearing H2228 crizotinib-resistant tumors EML4-ALK wild-type (WT; **A**), I1171T (**B**), C1156Y (**C**), or G1202R (**D**) were treated with 100 mg/kg crizotinib or 50 mg/kg ceritinib once daily for 12 to 22 days. Tumor volumes, mean ± SD ($n = 5$–8).

tumor that did not harbor an *ALK* resistance mutation, as this recapitulates observations in the clinic and with the patient-derived cell line shown in Fig. 3 (please see "Discussion").

Acquired Resistance to Ceritinib in Patients

Ceritinib has demonstrated impressive activity in the clinic in crizotinib-resistant patients (13). However, similar to other targeted therapy successes, despite initial and durable responses, tumors do develop resistance. We have now biopsied 11 cancers with acquired resistance to ceritinib (two of which were from different sites from the same patient). As shown in Fig. 6A, five of these biopsies revealed the development of mutations at either G1202 or F1174 in the ceritinib-resistant cancers. In the patient JFCR021, who had two sites of disease biopsied, two different ceritinib-resistant mutations were identified, underscoring the heterogeneity of resistance mechanisms that can be identified in a single patient (6). Of

Published OnlineFirst March 27, 2014; DOI: 10.1158/2159-8290.CD-13-0846

A

Patient ID	*EML4–ALK* sequence at crizotinib resistance	*EML4–ALK* sequence at ceritinib resistance
MGH011	S1206Y	G1202R
MGH015	WT	WT
MGH023	WT	F1174C
MGH034	WT	WT
MGH049	WT	WT
MGH051	WT	G1202R
MGH057	N/A	WT
MGH061	WT	WT
JFCR013	N/A	WT
JFCR021	G1269A (right lung)	F1174V (left lung) and G1202R (right lung)

B

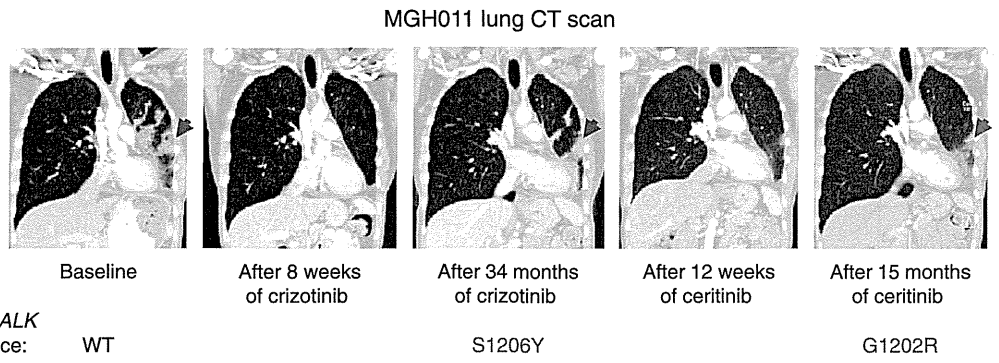

Figure 6. Ceritinib-resistant tumors acquired mutations at positions G1202 or F1174. **A,** ALK mutational status in ceritinib-resistant patient tumors before and after ceritinib treatment. **B,** thoracic computed tomography (CT) images of patient MGH011 during crizotinib or ceritinib treatments. Sites of biopsies (red arrows) revealed the presence of different *ALK* secondary mutations throughout the treatments. Tumor growth observed during ceritinib treatment is consistent with disease progression. WT, wild-type.

note, 2 of the patients had crizotinib-resistant mutations before enrolling on ceritinib (MGH011; Fig. 6B; and JFCR021) that our laboratory studies suggested would be sensitive to ceritinib. In the ceritinib-resistant cancers, those mutations were no longer detected, but the G1202R mutation emerged (Fig. 6B). These findings are consistent with preclinical studies presented in this article demonstrating the activity of ceritinib against G1269A and S1206Y crizotinib-resistant mutations, and its lack of potency against the G1202R mutation.

DISCUSSION

Since its approval in the United States in 2011, the ALK inhibitor crizotinib has emerged as a standard of care for patients with advanced NSCLC harboring the *ALK* fusion oncogene. Unfortunately, as has been observed with other targeted therapies, the emergence of resistance has ultimately limited the benefit of this therapy. Next-generation ALK inhibitors (ceritinib, CH5424802, ASP3026, AP26113, and X-396) have been developed with the hope that they may overcome acquired resistance to crizotinib. We previously reported differential activity of some of these ALK inhibitors depending on the resistance mutations present within the ALK TK domain (6, 11). In an ongoing early-phase clinical study, ceritinib has exhibited dramatic activity in patients with ALK-rearranged NSCLC (13).

In these studies, we find that ceritinib is a more potent ALK inhibitor than crizotinib, and has marked activity in crizotinib-naïve models of *ALK*-positive NSCLC, including H2228, H3122, and Ba/F3 cell lines *in vitro* and MGH006 primary explants *in vivo*. To better characterize the activity of ceritinib in crizotinib resistance, we developed a variety of crizotinib-resistant models, including cell lines derived from biopsies from patients whose cancers had developed resistance to crizotinib in the clinic. These models harbored different resistance mechanisms, including various *ALK* resistance mutations. The activity of ceritinib varied depending on the specific *ALK* resistance mutation. For example, in Ba/F3 models, ceritinib was highly active against L1196M, G1269A, S1206Y, and I1171T EML4–ALK mutants, and less active against the less common mutations C1156Y, G1202R, 1151T-ins, L1152P, and F1174C. It is notable that in the phase I

Published OnlineFirst March 27, 2014; DOI: 10.1158/2159-8290.CD-13-0846

study of ceritinib, five of 19 crizotinib-resistant tumors harbored resistance mutations at residues 1196, 1269, and 1206, with one tumor harboring both G1269A and 1151T-ins. The patients harboring these resistance mutations all exhibited significant tumor shrinkage (13).

Importantly, as has been observed in the clinic, ceritinib showed potent efficacy *in vitro* and *in vivo* against a crizotinib-resistant tumor that did not harbor an *ALK* resistance mutation or gene amplification (Fig. 3B). Interestingly, the patient-derived cell line also retained sensitivity to crizotinib *in vitro*, demonstrating that these cells are still sensitive to ALK inhibition. One potential explanation for this finding is that, in the clinic, crizotinib fails to achieve tumor levels that completely inhibit ALK, and that tumor cells can survive through modest input from activation of bypass tracks such as EGFR. However, these cells remain sensitive to complete ALK inhibition. In the setting of a more potent ALK inhibitor, ALK is inhibited fully, abrogating the functional role of bypass tracks and leading to the elimination of tumor cells. It is also possible that this patient relapsed on crizotinib because of poor adherence to therapy or due to a stromal contribution. Similar findings were also observed in the H2228 xenograft model that developed resistance to crizotinib *in vivo*, did not develop an *ALK* mutation, and was sensitive to ceritinib (Fig. 5A). These findings may explain, at least in part, the finding that ceritinib is highly active in crizotinib-resistant cancers with or without *ALK* resistance mutations.

The initial interrogation of ceritinib-resistant patient biopsies supports the notion that ceritinib is able to effectively suppress many crizotinib-resistant mutations, but the G1202R and F1174V/C mutants are resistant to ceritinib. It is noteworthy that in two cases, the crizotinib-resistant mutations, S1206Y and G1269A, were no longer observed in the ceritinib-resistant biopsies in which the G1202R mutations were observed (Fig. 6A). This suggests that predominant clones with the S1206Y and G1269A mutations were suppressed by ceritinib, whereas much more rare clones with G1202R mutations were selected by ceritinib. These findings give further support to the notion that there are multiple populations of resistant clones whose emergence is dependent on the selective pressure applied.

Altogether, our *in vitro* and *in vivo* data, including cell line models established from crizotinib-resistant patient samples, demonstrate that the next-generation ALK inhibitor ceritinib is active against most crizotinib-resistant tumors. This is consistent with the marked clinical activity of ceritinib in patients with *ALK*-positive NSCLC who progressed on crizotinib. As resistance to ceritinib has already been observed in the clinic, future studies will need to identify mechanisms of resistance to ceritinib other than mutations in the G1202 and F1174 residues to maximize the clinical benefit afforded by next-generation ALK-targeted therapies.

METHODS

Cell Lines and Reagents

All human lung cancer samples were obtained from patients with informed consent at the Massachusetts General Hospital (MGH) and the Japanese foundation for Cancer Research (JFCR), and all procedures were conducted under an Institutional Review Board (IRB)–approved protocol. Cells in pleural effusion were collected by centrifugation at 440 × *g* for 10 minutes. After red blood cells were lysed with the Red Blood Cell Lysis Solution (BioLegend), cells were grown in ACL-4 (Invitrogen) supplemented with 1% FBS or RPMI-1640 supplemented with 10% FBS and 1× Antibiotic-Antimycotic. After the cells started growing stably, clonal cell lines were also established.

H3122, H2228, A549, H460, H1299, HCC827, and H522 cell lines were provided by the Center for Molecular Therapeutics (CMT) at Massachusetts General Hospital (Boston, MA), which performs routine cell line authentication testing by single-nucleotide polymorphism and short-tandem repeat analysis. BT-474, SKBR3, and the *ALK*-positive patient-derived cell lines used in this study are from the Engelman laboratory (Boston, MA) and have been previously tested for mutation status to confirm their authenticity. A549, H460, H1299, HCC827, H522, SKBR3, H2228, H3122, H3122 CR1, and MGH021-4 cell lines were cultured in RPMI-1640 supplemented with 10% FBS. For survival assays, H2228 were cultured in 1% FBS. The MGH045 cell line was cultured in ACL-4 supplemented with 1% FBS, and MGH051 and BT-474 were cultured in DMEM supplemented with 10% FBS.

Mouse myeloma Ba/F3 cells were cultured in DMEM supplemented with 10% FBS with (parental) or without (EML4–ALK) IL3 (0.5 ng/mL). cDNAs encoding *EML4–ALK* variant1 or *EML4–ALK* variant3 containing different point mutations were cloned into retroviral expression vectors, and virus was produced as previously described (11). After retroviral infection, Ba/F3 cells were selected in puromycin (0.5 μg/mL) for 2 weeks. IL3 was withdrawn from the culture medium for more than 2 weeks before experiments.

Crizotinib was purchased from ChemieTek, and ceritinib was provided by Novartis. Both were dissolved in DMSO for *in vitro* experiments. Ceritinib was formulated in 0.5% methyl cellulose/0.5% Tween 80 and crizotinib in 0.1 N HCl or 0.5% methyl cellulose/0.5% Tween 80 for *in vivo* studies.

Western Blot Analysis

A total of 5×10^5 cells were treated in 6-well plates for 6 hours with the indicated drugs. Cell protein lysates were prepared as previously described (6, 11). Phospho-ERK (T202/Y204), ERK, S6, phospho-S6, phospho-AKT (S473 and T308), AKT, phospho-ALK (Y1282/1283), and ALK antibodies were obtained from Cell Signaling Technology. GAPDH was purchased from Millipore.

Survival Assays

Cells (2,000 or 5,000) were plated in triplicate into 96-well plates. Seventy-two hours (48 hours for Ba/F3 cells and 7 days for MGH051) after drug treatments, cells were incubated with a CellTiter-Glo assay reagent (Promega) for 15 minutes, and luminescence was measured with a Centro LB 960 Microplate Luminometer (Berthold Technologies).

In Vivo Efficacy Study of Ceritinib

SCID beige mice for crizotinib-resistant H2228 xenograft tumor models, nude mice for MGH006 primary explants and MGH045 cells were randomized into groups of 5, 6, or 8 mice with an average tumor volume of approximately 150 mm^3 and received crizotinib or ceritinib daily treatments by oral gavage as indicated in each study. Tumor volumes were determined by using caliper measurements and calculated with the formula (length × width × height)/2.

In Vitro Enzymatic Assay

An enzymatic assay for the recombinant ALK kinase domain (1066–1459) was conducted using the Caliper mobility shift methodology, using fluorescently labeled peptides as kinase substrates. The

Published OnlineFirst March 27, 2014; DOI: 10.1158/2159-8290.CD-13-0846

Caliper assay was performed at 30°C for 60 minutes in a total volume of 9 μL. The reaction was terminated by the addition of 16 μL of stop solution [100 mmol/L HEPES, 5% (v/v) DMSO, 0.1% (v/v) coating reagent, 10 mmol/L EDTA, 0.015% (v/v) Brij 35]. After termination of the reactions, the plates were transferred into the Caliper LabChip 3000 workstation for analysis.

Analysis of ALK/Ceritinib and ALK/Crizotinib Costructures

The ALK/ceritinib costructure was determined by the soaking of 2 mmol/L ceritinib into apo crystals grown in 0.2 mol/L sodium acetate trihydrate/20% PEG3350 using protein expressed and purified as previously described (18). The ALK/ceritinib final model determined to 2.0 Å (PDB 4MKC on hold) was superimposed with the coordinates of the ALK/crizotinib costructure (PDB 2XP2) for analyses.

Patient Sample Analyses

The patients with ALK-positive NSCLC with acquired ceritinib resistance underwent biopsy of their resistant tumors between January 2011 and September 2013. Standard histopathology was performed to confirm the diagnosis of malignancy as previously described (6). The electronic medical record was reviewed retrospectively to obtain clinical information under an IRB-approved protocol. This study was approved by the IRB of MGH or the Cancer Institute Hospital of JFCR.

Disclosure of Potential Conflicts of Interest

M. Nishio has received honoraria from the speakers' bureaus of Pfizer and Chugia Pharmaceutical Co., Ltd. A.T. Shaw is a consultant/advisory board member of Novartis, Pfizer, and ARIAD. J.A. Engelman has received commercial research grants from Novartis and Sanofi-Aventis, and is a consultant/advisory board member of Novartis, Sanofi-Aventis, Chugia Pharmaceutical Co., Ltd., and Ventana Medical Systems, Inc. No potential conflicts of interest were disclosed by the other authors.

Authors' Contributions

Conception and design: L. Friboulet, N. Li, P.-Y. Michellys, M.M. Awad, A.C. Pferdekamper, S. Kasibhatla, F. Sun, J.L. Harris, A.T. Shaw, J.A. Engelman

Development of methodology: L. Friboulet, R. Katayama, M.M. Awad, S. Kim, A.C. Pferdekamper, J. Li, S. Kasibhatla, F. Sun, S. Mahmood, E.L. Lockerman, N. Fujita

Acquisition of data (provided animals, acquired and managed patients, provided facilities, etc.): L. Friboulet, R. Katayama, C.C. Lee, J.F. Gainor, A.S. Crystal, N.Yanagitani, A.C. Pferdekamper, F. Sun, X. Sun, S. Hua, P. McNamara, M. Nishio, A.T. Shaw

Analysis and interpretation of data (e.g., statistical analysis, biostatistics, computational analysis): L. Friboulet, N. Li, R. Katayama, C.C. Lee, J.F. Gainor, M.M. Awad, N.Yanagitani, A.C. Pferdekamper, S. Kasibhatla, F. Sun, P. McNamara, J.L. Harris, A.T. Shaw, J.A. Engelman

Writing, review, and/or revision of the manuscript: L. Friboulet, N. Li, R. Katayama, C.C. Lee, J.F. Gainor, A.S. Crystal, M.M. Awad, J.L. Harris, A.T. Shaw, J.A. Engelman

Administrative, technical, or material support (i.e., reporting or organizing data, constructing databases): R. Katayama, A.C. Pferdekamper, S. Mahmood, E.L. Lockerman, N. Fujita, M. Nishio, J.A. Engelman

Study supervision: N. Li, S. Kasibhatla, M. Nishio, A.T. Shaw, J.A. Engelman

Acknowledgments

The authors thank Thomas Marsilje, Celin Tompkins, and Auzon Steffy for expert technical assistance and input on the studies described in the article; Atsushi Horiike for helping to obtain repeat biopsy samples; and Be a Piece of the Solution and the Evan Spirito Memorial Foundation for support of lung cancer research at MGH.

Grant Support

This work was supported by a grant from the NIH (5R01CA164273-02 to A.T. Shaw and J.A. Engelman), by a V Foundation Translational Research Grant (to A.T. Shaw and J.A. Engelman) and by the NIH/National Cancer Institute (R01CA137008 to J.A. Engelman). The study was also supported by a grant from JSPS KAKENHI (25710015 to R. Katayama).

Received November 5, 2013; revised March 12, 2014; accepted March 19, 2014; published OnlineFirst March 27, 2014.

REFERENCES

1. Kwak EL, Bang YJ, Camidge DR, Shaw AT, Solomon B, Maki R, et al. Anaplastic lymphoma kinase inhibition in non-small-cell lung cancer. N Engl J Med 2010;363:1693–703.
2. Soda M, Choi YL, Enomoto M, Takada S, Yamashita Y, Ishikawa S, et al. Identification of the transforming EML4-ALK fusion gene in non-small-cell lung cancer. Nature 2007;448:561–6.
3. Koivunen JP, Mermel C, Zejnullahu K, Murphy C, Lifshits E, Holmes AJ, et al. EML4-ALK fusion gene and efficacy of an ALK kinase inhibitor in lung cancer. Clin Cancer Res 2008;14:4275–83.
4. Doebele RC, Pilling AB, Aisner DL, Kutateladze TG, Le AT, Weickhardt AJ, et al. Mechanisms of resistance to crizotinib in patients with ALK gene rearranged non-small cell lung cancer. Clin Cancer Res 2012;18:1472–82.
5. Gainor JF, Varghese AM, Ou SH, Kabraji S, Awad MM, Katayama R, et al. ALK rearrangements are mutually exclusive with mutations in EGFR or KRAS: an analysis of 1,683 patients with non-small cell lung cancer. Clin Cancer Res 2013;19:4273–81.
6. Katayama R, Shaw AT, Khan TM, Mino-Kenudson M, Solomon BJ, Halmos B, et al. Mechanisms of acquired crizotinib resistance in ALK-rearranged lung Cancers. Sci Transl Med 2012;4:120ra117.
7. Choi YL, Soda M, Yamashita Y, Ueno T, Takashima J, Nakajima T, et al. EML4-ALK mutations in lung cancer that confer resistance to ALK inhibitors. N Engl J Med 2010;363:1734–9.
8. Lovly CM, Pao W. Escaping ALK inhibition: mechanisms of and strategies to overcome resistance. Sci Transl Med 2012;4:120ps122.
9. Sasaki T, Koivunen J, Ogino A, Yanagita M, Nikiforow S, Zheng W, et al. A novel ALK secondary mutation and EGFR signaling cause resistance to ALK kinase inhibitors. Cancer Res 2011;71:6051–60.
10. Sasaki T, Okuda K, Zheng W, Butrynski J, Capelletti M, Wang L, et al. The neuroblastoma-associated F1174L ALK mutation causes resistance to an ALK kinase inhibitor in ALK-translocated cancers. Cancer Res 2010;70:10038–43.
11. Katayama R, Khan TM, Benes C, Lifshits E, Ebi H, Rivera VM, et al. Therapeutic strategies to overcome crizotinib resistance in non-small cell lung cancers harboring the fusion oncogene EML4-ALK. Proc Natl Acad Sci U S A 2011;108:7535–40.
12. Marsilje TH, Pei W, Chen B, Lu W, Uno T, Jin Y, et al. Synthesis, structure-activity relationships, and *in vivo* efficacy of the novel potent and selective anaplastic lymphoma kinase (ALK) inhibitor 5-Chloro-N2-(2-isopropoxy-5-methyl-4-(piperidin-4-yl)phenyl)-N4-(2-(isopropylsulfonyl)phenyl)pyrimidine-2,4-diamine (LDK378) currently in phase 1 and phase 2 clinical trials. J Med Chem 2013;56:5675–90.
13. Shaw AT, Kim DW, Mehra R, Tan DS, Felip E, Chow LQ, et al. Ceritinib in ALK-rearranged non-small-cell lung cancer. N Engl J Med 2014;370:1189–97.
14. Early Results Promising for LKD378 in ALK-positive NSCLC. Cancer Discov 2013;3:OF5.
15. FDA, Center for Drug Evaluation and Research. 2011Application Number: 202570Orig1s000; Reference ID: 3006911.
16. Cui JJ, Tran-Dube M, Shen H, Nambu M, Kung PP, Pairish M, et al. Structure based drug design of crizotinib (PF-02341066), a potent